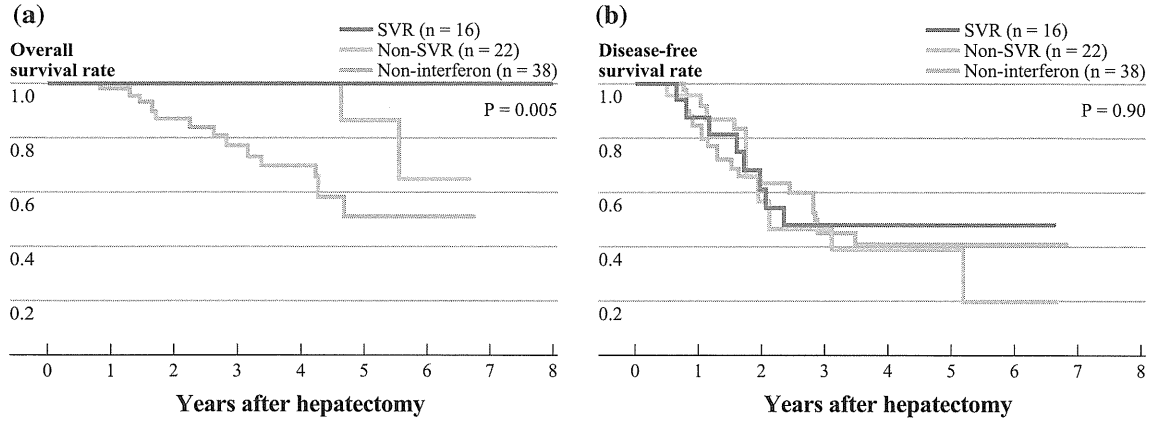

FIG. 2 Overall survival and disease-free survival of patients with hepatitis C-related HCC with respect to SVR after IFN therapy

intrahepatic recurrences (more than four nodules) was significantly lower in the peg-IFN group than in the non-IFN group ($P = 0.0047$). The proportion of patients in whom surgery or RFA was selected for treatment was significantly higher in the peg-IFN group than in the non-IFN group ($P = 0.0346$). Furthermore, regarding re-recurrence of HCC after treatment of the first-recurrent HCC, the 1-year disease-free survival rates of patients after treatment of the first-recurrent HCC was 48.5% in patients ($n = 21$) who received peg-IFN therapy and 12.5% in patients ($n = 17$) who did not receive IFN therapy. There was a statistically significant difference in disease-free survival between the two groups ($P = 0.0012$) (Fig. 3).

A comparison of results of the preoperative liver function test with those of postoperative 1-year liver function tests is presented in Table 3. In patients who received peg-IFN therapy, total bilirubin levels 1 year after surgery were significantly decreased compared with preoperative total bilirubin levels ($P = 0.018$), whereas in patients who did not receive IFN therapy, the total bilirubin level at 1 year after surgery was similar to the total bilirubin level before surgery ($P = 0.107$).

TABLE 2 Recurrence and treatments for recurrence after hepatic resection

	Peg-IFN (+) ($n = 38$)	IFN (−) ($n = 38$)	*P* value
HCC recurrence[a]: yes	21 (55.3%)	17 (44.7%)	0.359
Pattern of recurrence[b]			0.0047
Intrahepatic (single)	9 (42.9%)	8 (47.1%)	
Intrahepatic (2–3)	10 (47.6%)	1 (5.9%)	
Intrahepatic (multiple)	2 (9.5%)	8 (47.1%)	
Main modalities[b]			0.0346
Repeat hepatectomy	8 (38.1%)	2 (11.8%)	
RFA	8 (38.1%)	4 (23.5%)	
TACE	5 (23.8%)	11 (64.7%)	

peg-IFN pegylated interferon, *RFA* radiofrequency ablation, *TACE* transcatheter arterial chemoembolization

[a] Data expressed as number of patients (percentage of total patients)

[b] Data expressed as number of patients (percentage of patients who had a recurrence)

DISCUSSION

Our results revealed that peg-IFN therapy after hepatic resection improved the outcomes of HCV patients, although the interval of disease-free survival was not prolonged. Peg-IFN therapy after hepatectomy improved hepatic reserve function and suppressed multiple HCC recurrences (more than four nodules). Furthermore, re-recurrence after treatment of first-recurrent HCC after hepatic resection was significantly suppressed in the peg-IFN group compared with that in the non-IFN group. IFN has been reported to exert antitumor effects. IFN increases natural killer cell activity and exhibits antiangiogenic properties.[35,36] IFN has also been reported to be effective in eradicating HCV RNA

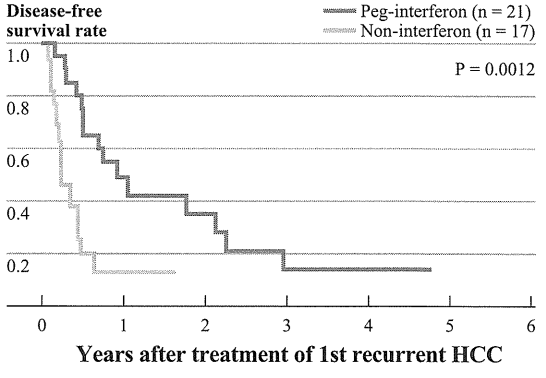

FIG. 3 Comparison of disease-free survival rate after treatment of first-recurrent HCC in patients who received peg-IFN therapy or in those who did not receive IFN therapy

TABLE 3 Comparison of preoperative liver function with 1-year liver function after hepatic resection

	Peg-IFN (+)		*P* value	IFN (−)		*P* value
	Preoperative	1 Year after surgery		Preoperative	1 Year after surgery	
T-Bil (mg/dl)	0.82 ± 0.29	0.71 ± 0.26	0.0189	0.81 ± 0.32	0.92 ± 0.35	0.107
AST (IU/l)	50.1 ± 24.1	45.8 ± 23.5	0.310	42.1 ± 18.9	56.1 ± 26.7	0.0110
ALT (IU/l)	51.3 ± 28.6	36.4 ± 22.8	0.00809	40.3 ± 24.3	49.7 ± 25.8	0.0918
Albumin (g/dl)	3.89 ± 0.80	3.99 ± 0.71	0.251	3.73 ± 0.45	3.75 ± 0.44	0.807

peg-IFN pegylated interferon, *AST* aspartate aminotransferase, *ALT* alanine aminotransferase

from serum and hepatic tissue, thereby preventing deterioration of liver function in patients with HCV infection.[37] IFN prevents worsening of compensated cirrhosis.[18,37] Our results are compatible with those reported in those studies. In the peg-IFN group, most patients with HCC recurrence could undergo curative treatments such as repeat hepatectomy or RFA as a recurrence treatment, because the number of recurrent tumors was usually limited to three. IFN therapy appears to increase survival not only by improving residual liver function and increasing the possibility of radical treatment of recurrences but also by suppressing re-recurrence after the first recurrence of HCC.

The current study also revealed that the overall survival of patients with SVR was significantly better than that of patients without SVR. This result suggests that IFN prolongs the outcomes of patients with HCC after hepatic resection by causing remission of active hepatitis and eradication of HCV RNA in patients who attained SVR after hepatic resection.

In this study, to clarify the impact of peg-IFN therapy on outcomes of HCV-related HCC after hepatic resection, patients who received IFNs such as IFN-α or IFN-β were excluded. RCTs investigating adjuvant effects of IFN after resection or ablation of HCC were performed using IFN-α. Few studies have investigated the effects of peg-IFN plus RBV combination therapy on survival and recurrence after curative resection of HCC. Combination therapy with peg-IFN and RBV has recently been developed, and peg-IFN therapy has resulted in significantly higher SVR rates and better tolerability than treatment with IFN-α.[21,23] In our study, incidence of SVR after hepatic resection was 42.1%, which was higher than that in previous studies that reported an SVR rate of 0–10%.[12–14] The compliance of patients to peg-IFN therapy observed in the present study (68.4%) was higher than that reported elsewhere (approximately 40%).[14] This enhanced efficacy of the peg-IFN formulations might contribute to the prolonged survival of HCC patients after hepatic resection.

In this study, HCC patients who received peg-IFN therapy within 9 months after surgery were enrolled, and HCC patients who experienced recurrence of HCC within 9 months after hepatic resection were excluded from the non-IFN group, because these patients could lose the opportunity to receive IFN therapy for HCC recurrence on being assigned to the peg-IFN therapy group.

Before matching by using the propensity score, the clinical characteristics of the entire study population that can strongly influence outcomes differed significantly between the peg-IFN group and non-IFN group. The proportion of older patients was higher in the non-IFN group than in the peg-IFN group, whereas the proportion of patients who had longer operation times tended to be lower in the non-IFN group than in the peg-IFN group. To overcome bias due to the different distribution of the severity of liver function impairment between the two groups, a one-to-one match was created using propensity score analysis. After matching by propensity score, prognostic variables were appropriately handled, and there was no significant difference in prognostic factors between the two matched groups. This study had a limitation related to the small sample size after propensity score matching. To overcome this, further examination with larger sample sizes is necessary, and the potential efficacy of peg-IFN therapy must be validated in larger prospective RCTs.

CONCLUSIONS

Several previous RCTs investigating the effects of IFN on survival and tumor recurrence after hepatic resection were inconclusive. However, in the current study, peg-IFN therapy following hepatic resection improved the survival rates of hepatectomized patients with HCV-related HCC. The results of this study suggest that peg-IFN therapy is effective as an adjuvant chemopreventive agent after hepatic resection in patients with HCV-related HCC.

ACKNOWLEDGMENT The authors thank Prof. Junko Tanaka of the Department of Epidemiology, Infectious Disease Control and Prevention, Hiroshima University, for assistance in performing the propensity score analysis.

CONFLICT OF INTEREST The authors have no commercial associations (e.g., consultancies, stock ownership, equity interest, patent/licensing arrangements) that might pose a conflict of interest related to the submitted manuscript.

REFERENCES

1. Poon RTP, Fan ST, Lo CM, Liu CL, Wong J. Intrahepatic recurrence after curative resection of hepatocellular carcinoma: long-term results of treatment and prognostic factors. *Ann Surg*. 1999;229:216–22.
2. Minagawa M, Makuuchi M, Takayama T, Kokudo N. Selection criteria for repeat hepatectomy in patients with recurrent hepatocellular carcinoma. *Ann Surg*. 2003;238:703–10.
3. Itamoto T, Nakahara H, Amano H, et al. Repeat hepatectomy for recurrent hepatocellular carcinoma. *Surgery*. 2007;141:589–97.
4. Ikeda K, Saitoh S, Arase Y, Chayama K, et al. Effects of interferon therapy on hepatocellular carcinogenesis in patients with chronic hepatitis type C: a long-term observation study of 1,643 patients using statistical bias correction with proportional hazard analysis. *Hepatology*. 1999;29:1124–30.
5. Imai Y, Kawata S, Tamura S, et al. Relation of interferon therapy and hepatocellular carcinoma in patients with chronic hepatitis C. Osaka Hepatocellular Carcinoma Prevention Study Group. *Ann Intern Med*. 1998;129:94–9.
6. Camma C, Giunta M, Andreone P, Craxì A. Interferon and prevention of hepatocellular carcinoma in viral cirrhosis: an evidence-based approach. *J Hepatol*. 2001;34:593–602.
7. Nishiguchi S, Shiomi S, Nakatani S, et al. Prevention of hepatocellular carcinoma in patients with chronic active hepatitis C and cirrhosis. *Lancet*. 2001;357:196–7.
8. Tomimaru Y, Nagano H, Eguchi H, et al. Effects of preceding interferon therapy on outcome after surgery for hepatitis C virus-related hepatocellular carcinoma. *J Surg Oncol*. 2010;102:308–14.
9. Jeong SC, Aikata H, Katamura Y, et al. Low-dose intermittent interferon-alpha therapy for HCV-related liver cirrhosis after curative treatment of hepatocellular carcinoma. *World J Gastroenterol*. 2007;13:5188–95.
10. Jeong SC, Aikata H, Kayamura Y, et al. Effects of a 24-week course of interferon-α therapy after curative treatment of hepatitis C virus-associated hepatocellular carcinoma. *World J Gastroenterol*. 2007;13:5343–50.
11. Harada H, Kitagawa M, Tanaka N, et al. Anti-oncogenic and oncogenic potentials of interferon regulatory factors-1 and -2. *Science*. 1993;259:971–4.
12. Liedtke C, Grogner N, Manns MP, Trautwein C. Interferon-alpha enhances TRAIL-mediated apoptosis by up-regulating caspase-8 transcription in human hepatoma cells. *J Hepatol*. 2006;44:342–9.
13. Kubo S, Nishiguchi S, Hirohashi K, Tanaka H, Shuto T, Kinoshita H. Randomized clinical trial of long-term outcome after resection of hepatitis C virus-related hepatocellular carcinoma by postoperative interferon therapy. *Br J Surg*. 2002;89:418–22.
14. Ikeda K, Arase Y, Saitoh S, et al. Interferon beta prevents recurrence of hepatocellular carcinoma after complete resection or ablation of primary tumor-a prospective randomized study of hepatitis C virus-related liver cancer. *Hepatology*. 2000;32:228–32.
15. Mazzaferro V, Romito R, Schiavo M, et al. Prevention of hepatocellular carcinoma recurrence with alpha-interferon after liver resection in HCV cirrhosis. *Hepatology*. 2006;44:1543–54.
16. Lo CM, Liu CL, Chan SC, et al. A randomized, controlled trial of postoperative adjuvant interferon therapy after resection of hepatocellular carcinoma. *Ann Surg*. 2007;245:831–42.
17. Manns MP, McHutchison JG, Gordon SC, et al. Peginterferon alfa-2b plus ribavirin compared with interferon alfa-2b plus ribavirin for initial treatment of chronic hepatitis C: a randomized trial. *Lancet*. 2001;358:958–65.
18. Fried MW, Shiffman ML, Rajender Reddy K, et al. Peginterferon alfa-2a plus ribavirin for chronic hepatitis C virus infection. *N Engl J Med*. 2002;347:975–82.
19. Yoshida H, Arakawa Y, Sata M, et al. Interferon therapy prolonged life expectancy among chronic hepatitis C patients. *Gastroenterology*. 2002;123:483–91.
20. Kiyosawa K, Uemura T, Ichijo T, et al. Hepatocellular carcinoma: recent trends in Japan. *Gastroenterology*. 2004;127:S17–26.
21. McHutchison JG, Gordon SC, Schiff ER, et al. Interferon alfa-2b alone or in combination with ribavirin as initial treatment for chronic hepatitis C. Hepatitis Interventional Therapy Group. *N Engl J Med*. 1998;339:1485–92.
22. Muir AJ, Bornstein JD, Killenberg PG. Peginterferon alfa-2b and ribavirin for the treatment of chronic hepatitis C in blacks and non-Hispanic whites. *N Eng J Med*. 2004;350:2265–71.
23. Shirakawa H, Matsumoto A, Joshita S, et al. Pretreatment prediction of virological response to peginterferon plus ribavirin therapy in chronic hepatitis c patients using viral and host factors. *Hepatology*. 2008;48:1753–60.
24. Kogure T, Ueno Y, Fukushima K, et al. Pegylated interferon plus ribavirin for genotype 1b chronic hepatitis C in Japan. *World J Gastroentrol*. 2008;14:7225–30.
25. Liver Cancer Study Group of Japan. General Rules for the Clinical and Pathological Study of Primary Liver Cancer. 5th ed. Tokyo: Kanehara; 2008.
26. Itamoto T, Nakahara H, Tashiro H, et al. Indications of partial hepatectomy for transplantable hepatocellular carcinoma with compensated cirrhosis. *Am J Surg*. 2005;189:167–72.
27. Oishi K, Itamoto T, Kobayashi T, et al. Hepatectomy for hepatocellular carcinoma in elderly patients aged 75 years or more. *J Gastrointest Surg*. 2009;13:695–701.
28. Makuuchi M, Hasegawa H, Yamazaki S. Ultrasonically guided subsegmentectomy. *Surg Gynecol Obstet*. 1985;161:346–50.
29. Yamamoto M, Takasaki K, Otsubo T, et al. Favorable surgical outcomes in patients with early hepatocellular carcinoma. *Ann Surg*. 2004;239:395–9.
30. Itamoto T, Katayama K, Nakahara H, Tashiro H, Asahara T. Autologous blood storage before hepatectomy for hepatocellular carcinoma with underlying liver disease. *Br J Surg*. 2003;90:23–8.
31. Clavien PA, Barkun J, de Oliveira ML, et al. The Clavien–Dindo classification of surgical complications: five-year experience. *Ann Surg*. 2009;250:187–96.
32. Zinsmeister AR, Connor JT. Ten common statistical errors and how to avoid them. *Am J Gastroenterol*. 2008;103:262–6.
33. Rosenbaum PR, Rubin DB. The central role of the propensity score in observational studies for causal effects. *Biometrika*. 1983;70:41–55.
34. Rubin DB. Estimating causal effects from large data sets using propensity scores. *Ann Intern Med*. 1997;127:757–63.
35. D'Agostino RB Jr. Propensity score methods for bias reduction in the comparison of a treatment to non-randomized control group. *Stat Med*. 1998;17:2265–81.
36. Brinkmann V, Geiger T, Alkan S, Heusser CH. Interferon alpha increases the frequency of interferon gamma-producing human CD4+T cells. *J Exp Med*. 1993;178:1655–63.
37. Wang L, Tang ZY, Qin LX, et al. High-dose and long-term therapy with interferon-alfa inhibits tumor growth and recurrence in nude mice bearing human hepatocellular carcinoma xenografts with high metastatic potential. *Hepatology*. 2000;32:43–8.
38. Shiratori Y, Shiina S, Teratani T, et al. Interferon therapy after tumor ablation improves prognosis in patients with hepatocellular carcinoma associated with hepatitis C. *Ann Intern Med*. 2003;138:299–306.

nature medicine

Identification of the Niemann-Pick C1–like 1 cholesterol absorption receptor as a new hepatitis C virus entry factor

Bruno Sainz Jr[1], Naina Barretto[1], Danyelle N Martin[2], Nobuhiko Hiraga[3], Michio Imamura[3], Snawar Hussain[1], Katherine A Marsh[2], Xuemei Yu[1,5], Kazuaki Chayama[3], Waddah A Alrefai[1,4] & Susan L Uprichard[1,2]

Hepatitis C virus (HCV) is a leading cause of liver disease worldwide. With ~170 million individuals infected and current interferon-based treatment having toxic side effects and marginal efficacy, more effective antivirals are crucially needed[1]. Although HCV protease inhibitors were just approved by the US Food and Drug Administration (FDA), optimal HCV therapy, analogous to HIV therapy, will probably require a combination of antivirals targeting multiple aspects of the viral lifecycle. Viral entry represents a potential multifaceted target for antiviral intervention; however, to date, FDA-approved inhibitors of HCV cell entry are unavailable. Here we show that the cellular Niemann-Pick C1–like 1 (NPC1L1) cholesterol uptake receptor is an HCV entry factor amendable to therapeutic intervention. Specifically, NPC1L1 expression is necessary for HCV infection, as silencing or antibody-mediated blocking of NPC1L1 impairs cell culture–derived HCV (HCVcc) infection initiation. In addition, the clinically available FDA-approved NPC1L1 antagonist ezetimibe[2,3] potently blocks HCV uptake *in vitro* via a virion cholesterol–dependent step before virion-cell membrane fusion. Moreover, ezetimibe inhibits infection by all major HCV genotypes *in vitro* and *in vivo* delays the establishment of HCV genotype 1b infection in mice with human liver grafts. Thus, we have not only identified NPC1L1 as an HCV cell entry factor but also discovered a new antiviral target and potential therapeutic agent.

HCV is thought to enter cells via receptor-mediated endocytosis beginning with interaction of the viral particle with a series of cell surface receptors, including the tetraspanin CD81 protein[4], scavenger receptor class B member I (SR-BI, also known as SCARB1)[5] and the tight-junction proteins claudin-1 (CLDN1)[6] and occludin (OCLN)[7,8], followed by clathrin-mediated endocytosis and fusion between the virion envelope and the endosomal membrane[9,10]. Although the specifics of each interaction are not fully understood, it is now recognized that multiple cellular factors, as well as many components of the viral particle, not just the viral glycoproteins, participate in the entry process. For example, the HCVcc particle is associated with cellular lipoproteins (for example, low-density lipoprotein and very-low-density lipoprotein)[11,12] and is enriched in cholesterol[13], the latter of which has been shown to be necessary for HCV cell entry[13,14]. Apart from the likely function of cholesterol in viral membrane stabilization and organization, the dependence of HCV infectivity on cholesterol led us to reason that other cholesterol-uptake receptors (apart from SR-BI and LDLR), such as NPC1L1, might also have a role in HCV cell entry.

NPC1L1, a 13-transmembrane-domain cell surface cholesterol-sensing receptor (**Fig. 1a**) expressed on the apical surface of intestinal enterocytes and human hepatocytes, including Huh7 cells (**Supplementary Fig. 1**), is responsible for cellular cholesterol absorption and whole-body cholesterol homeostasis[15,16]. Similar to what has been observed for other HCV entry factors[8], we observed downregulation of NPC1L1 in HCVcc-infected Huh7 cultures. Specifically, as early as day 4 after infection NPC1L1 protein levels were markedly reduced and remained downregulated until the end of the experiment at day 12 after infection (**Fig. 1b**). Having observed a correlation between NPC1L1 expression and HCV infection, we next determined whether NPC1L1 expression levels affect HCV infection by transfecting Huh7 cells with siRNAs targeting NPC1L1 or the known HCV entry factors CD81 or SR-BI. Compared to cells transfected with an irrelevant control siRNA, CD81-, SR-BI- and NPC1L1-silenced cells were significantly less susceptible to HCVcc infection (**Fig. 1c**). The inhibition was HCV specific, as silencing of these proteins had no effect on vesicular stomatitis virus G protein–pseudotyped particle (VSVGpp) infection (**Supplementary Fig. 2a**). Inhibition of HCV also correlated with a reduction in NPC1L1 mRNA and protein and was NPC1L1 specific and not the result of off-target effects (**Fig. 1d,e**, **Supplementary Figs. 3** and **4a,b**). Although protein amounts were only marginally lowered by siRNA knockdown, the effect on HCV was considerable, highlighting the sensitivity of HCV to small changes in NPC1L1 levels. Notably, SR-BI mRNA expression has been shown to be reduced by NPC1L1 knockdown in nonhepatic cells[17] and SR-BI is an HCV entry factor[5], but we found that SR-BI expression was not adversely affected by NPC1L1 silencing in Huh7 cells (**Supplementary Fig. 4c,d**). Finally, NPC1L1 silencing had no effect on HCV subgenomic RNA replication, full-length infectious HCVcc RNA replication or secretion of *de novo* HCVcc (**Supplementary Fig. 5**).

[1]Department of Medicine, University of Illinois–Chicago, Chicago, Illinois, USA. [2]Department of Microbiology and Immunology, University of Illinois–Chicago, Chicago, Illinois, USA. [3]Department of Medicine and Molecular Science, Graduate School of Biomedical Sciences, Hiroshima University, Hiroshima, Japan. [4]Digestive Disease and Nutrition, Jesse Brown Virginia Medical Center, Chicago, Illinois, USA. [5]Current address: Kadmon Corporation, New York, New York, USA. Correspondence should be addressed to B.S. (bsainz@uic.edu) or S.L.U. (sluprich@uic.edu).

Received 16 March 2011; accepted 25 October 2011; published online 8 January 2012; doi:10.1038/nm.2581

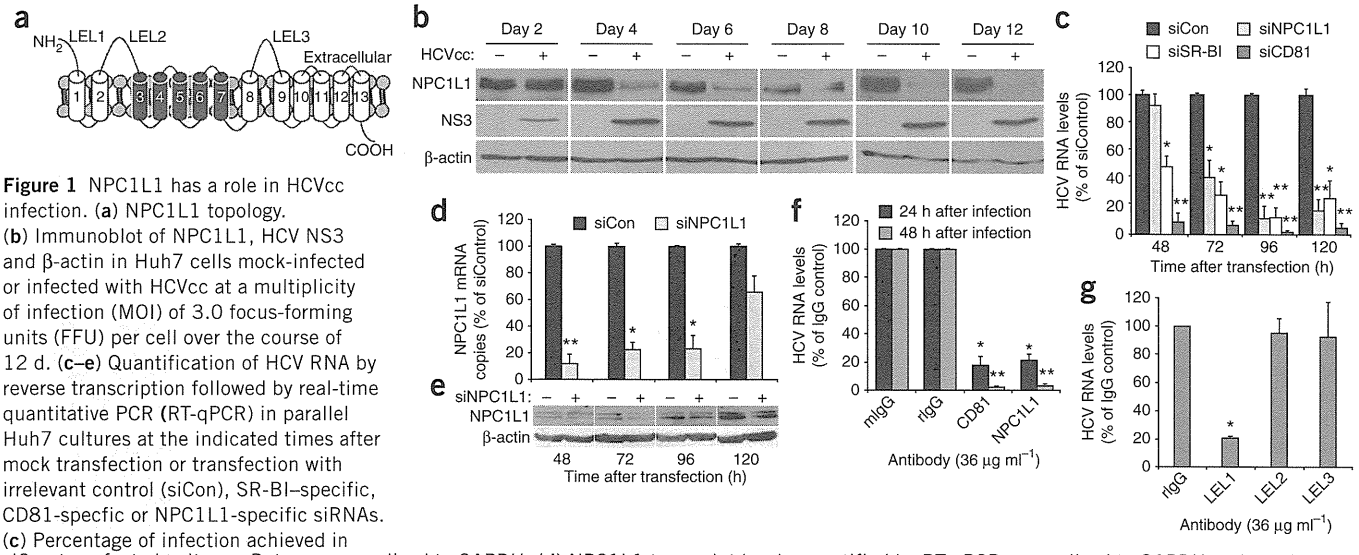

Figure 1 NPC1L1 has a role in HCVcc infection. (**a**) NPC1L1 topology. (**b**) Immunoblot of NPC1L1, HCV NS3 and β-actin in Huh7 cells mock-infected or infected with HCVcc at a multiplicity of infection (MOI) of 3.0 focus-forming units (FFU) per cell over the course of 12 d. (**c–e**) Quantification of HCV RNA by reverse transcription followed by real-time quantitative PCR (RT-qPCR) in parallel Huh7 cultures at the indicated times after mock transfection or transfection with irrelevant control (siCon), SR-BI–specific, CD81-specfic or NPC1L1-specific siRNAs. (**c**) Percentage of infection achieved in siCon-transfected cultures. Data are normalized to GAPDH. (**d**) NPC1L1 transcript levels quantified by RT-qPCR, normalized to GAPDH and graphed as a percentage of the maximum number of copies determined in siCon-transfected cultures at each time point examined. (**e**) Immunoblot of NPC1L1 and β-actin protein in siCon-transfected (–) and siNPC1L1-transfected cultures (+). (**f,g**) Intracellular HCV RNA levels detected in parallel Huh7 cell cultures treated with 36 μg ml^{-1} of a mouse (mIgG) or rabbit (rIgG) isotype control antibody, a CD81-specific antibody or antibodies specific for each of the three LELs of NPC1L1 for 1 h before and during HCVcc infection. Shown are HCV RNA levels, determined by RT-qPCR and normalized to GAPDH levels, 24 h (**f**) or 48 h (**f,g**) after infection. Results are graphed as a percentage of infection achieved in the respective IgG control-treated cultures. In all cases, significant differences relative to controls (one-way analysis of variance (ANOVA) and Tukey's post-hoc *t* test) are denoted as $^*P < 0.05$ or $^{**}P < 0.01$. All results are graphed as means ± s.d. for triplicate samples. The data presented are representative of three independent experiments.

Because siRNA-mediated knockdown of NPC1L1 suggested that HCV infection is inhibited at a step before RNA replication or secretion, we next assessed whether HCV infection was susceptible to inhibition by antibody-mediated blocking of cell surface NPC1L1. Compared to cells treated with irrelevant IgG control antibodies, HCVcc infection, as measured by intracellular HCV RNA levels, was significantly reduced in cells treated with an antibody specific for the known HCV cell entry factor CD81 (**Fig. 1f**). When we incubated cells with an NPC1L1-specific antibody, HCVcc infection was similarly reduced (**Fig. 1f**), and the inhibition was HCV specific, as antibody-mediated blocking had no effect on VSVGpp entry (**Supplementary Fig. 2b,c**). To determine the NPC1L1 domains necessary for HCV entry, we treated cells with antibodies targeting each of the three large extracellular loops (LELs) of NPC1L1 and observed that HCV infection was reduced only when NPC1L1 LEL1, but not LEL2 or LEL3, was blocked (**Fig. 1g**). Thus, NPC1L1 silencing and antibody-mediated blocking of NPC1L1 LEL1 reduced HCV infection as effectively as targeting other known HCV cell entry factors.

Ezetimibe is a 2-azetidinone–class drug that has been approved by the FDA as a cholesterol-lowering medication[18]. As ezetimibe has been shown to be a direct inhibitor of NPC1L1 internalization[19,20], we next used this high-affinity, specific pharmacological agent as an alternate means of targeting NPC1L1 before, during or after viral inoculation while additionally evaluating its anti-HCV potential. Specifically, we performed HCVcc foci-reduction assays and quantified foci (that is, clusters of ≥5 HCV E2–positive cells) after ezetimibe treatment. Ezetimibe reduced HCVcc foci formation in a dose-dependent manner when present before infection and then removed (**Fig. 2a**) or only during virus inoculation (**Fig. 2b**). However, when we added ezetimibe to cells after inoculation (**Fig. 2c**), the initiation of HCV-positive foci was unaffected, as would be expected for a viral entry inhibitor. Notably, the highest dose of ezetimibe (25 μM) reduced the size of the HCV-positive foci observed from the typical ≥5 HCV E2–positive cells to only 1–3 HCV E2–positive cells per focus, which accounts for the lower number of foci with ≥5 HCV E2-positive cells being counted in those cultures, suggesting that NPC1L1 may also affect HCV cell-to-cell spread (data not shown). Dose-responsive, time-of-addition–dependent inhibition of HCV infection was also evident when HCV RNA levels were measured (**Supplementary Fig. 6**). We additionally observed ezetimibe sensitivity across a panel of HCVcc intergenotypic clones containing the structural regions of diverse HCV genotypes (1 – 7)[21] (**Fig. 2d**). Finally, because NPC1L1 and SR-BI are both involved in cellular cholesterol uptake and SR-BI has been reported to be a rate-limiting HCV cell entry factor[22], we overexpressed SR-BI before ezetimibe treatment and found that this overexpression did not overcome the dependence of HCV entry on NPC1L1 (**Supplementary Fig. 7**). Likewise, we confirmed that the potent antiviral effect of ezetimibe was not due to drug-mediated cytotoxicity (**Supplementary Figs. 2d,e** and **8a**), changes in cell proliferation (**Supplementary Fig. 8b**), reduced expression of the other known HCV cell surface receptors (**Supplementary Fig. 8c–g**), inhibition of HCV RNA replication (**Supplementary Fig. 9a–c**) or inhibition of virus secretion (**Supplementary Fig. 9d**). Hence, the data support the conclusion that direct pharmacological inhibition of NPC1L1 reduces HCV infection by directly inhibiting viral cell entry.

We next assessed whether ezetimibe inhibits HCVcc binding or a post-binding step by examining cell-associated HCV RNA and protein expression from internalized RNA in vehicle- and ezetimibe-treated HCVcc-infected cultures. At 10 h after infection, a time before detectable HCV RNA replication occurs (**Supplementary Fig. 10**), ezetimibe did not affect cell-bound HCV RNA levels (**Fig. 2e**). In contrast, at later time points, HCV RNA levels (**Fig. 2e**) and *de novo* NS5A protein expression (**Fig. 2f,g**) were reduced in ezetimibe-treated cultures, suggesting HCV can efficiently bind ezetimibe-treated cells, but a post-binding step is prevented. To further test this hypothesis

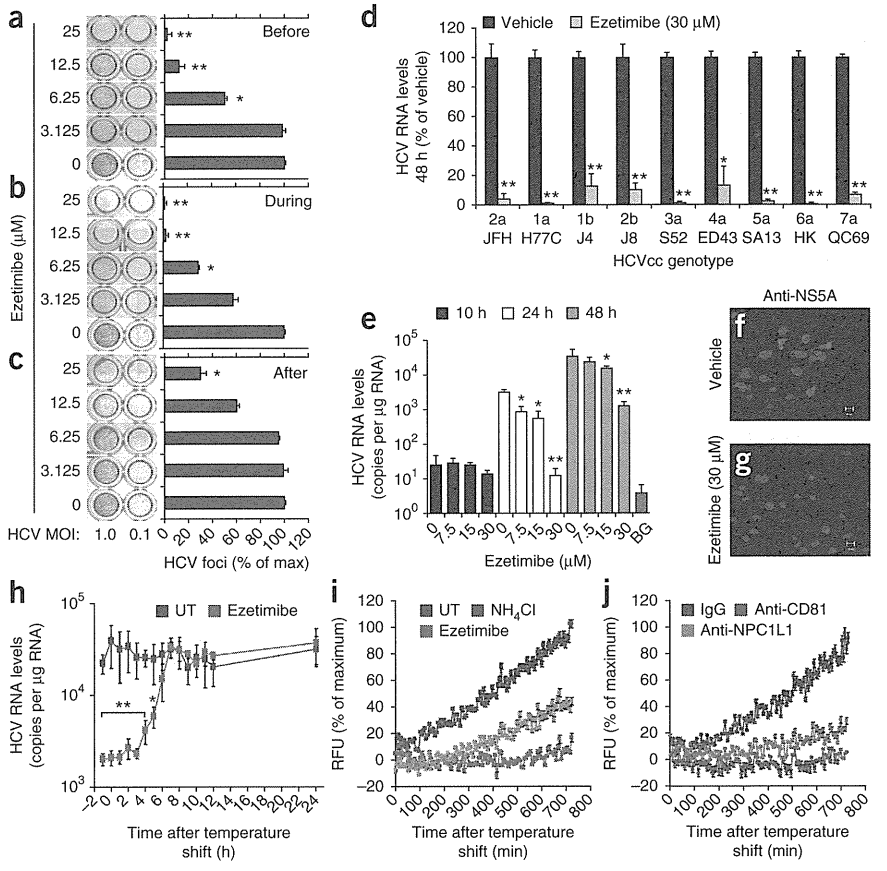

Figure 2 Ezetimibe-mediated inhibition of NPC1L1 reduces HCV entry at a post-binding, prefusion step. (**a**–**c**) Quantification of HCV foci observed in Huh7 cultures treated with vehicle or increasing concentrations of ezetimibe for 6 h before infection and then removed (Before) (**a**), for 12 h coincident with viral inoculation and then removed (During) (**b**) or after viral inoculation (After) (**c**). HCV foci are expressed as a percentage of the foci obtained in vehicle-treated (0 μM) cultures ± s.d. ($n = 3$). MOI, multiplicity of infection. (**d**,**e**) Intracellular HCV RNA levels detected in parallel Huh7 cultures treated with vehicle or the indicated concentrations of ezetimibe beginning 1 h before and during infection with HCVcc containing the structural region of the indicated genotypes (**d**) or HCVcc JFH-1 (**e**). Shown are HCV RNA levels, determined by RT-qPCR and normalized to GAPDH, at the indicated times after infection. Results are graphed as a percentage of infection in vehicle-treated cultures or as mean HCV RNA copies per μg total cellular RNA ± s.d. ($n = 3$). Assay background (BG) is the HCV RNA level detected in uninfected samples. (**f**,**g**) Indirect immunofluorescence analysis of HCV NS5A in vehicle-treated (**f**) and ezetimibe-treated (30 μM) (**g**) cultures 24 h after infection with HCVcc JFH-1. Scale bars, 20 μm. (**h**) Intracellular HCV RNA levels detected in synchronized infections performed in parallel Huh7 cultures treated with vehicle or ezetimibe (30 μM) at the indicated times. Shown are HCV RNA levels, determined by RT-qPCR and normalized to GAPDH, 30 h after infection. Results are graphed as mean HCV RNA copies per μg total cellular RNA ± s.d. ($n = 3$). $^*P < 0.05$ or $^{**}P < 0.01$ for HCV relative to vehicle-treated cultures (one-way ANOVA and Tukey's post-hoc t test). (**i**,**j**) HCV fusion, as measured by DiD fluorescence dequenching in Huh7 cells treated with vehicle (UT), NH_4Cl (10 mM), ezetimibe (30 μM), IgG control antibody (36 μg ml^{-1}), CD81-specific antibody (anti-CD81, 36 μg ml^{-1}), or an antibody to NPC1L1 LEL1 (anti-NPC1L1, 36 μg ml^{-1}). Results are graphed as a percentage of maximum background-corrected relative fluorescence units (RFU) achieved in vehicle-treated or IgG control-treated cultures. All data presented are representative of three independent experiments.

and determine when during the entry process NPC1L1 functions, we assessed the ability of ezetimibe to block HCVcc infection when added at various times after virus binding at 4 °C. Ezetimibe retained inhibitory activity after temperature shift to 37 °C for up to 5 h (half-maximal inhibition at 4 h), confirming that NPC1L1 functions after binding, probably late in viral entry (**Fig. 2h**).

To determine whether ezetimibe acts before fusion, we developed a fluorescence-based HCVcc fusion assay. Specifically, we labeled HCVcc with the hydrophobic fluorophore DiD[23], which incorporates into biological membranes and, at high concentrations, is self-quenching. Upon fusion of viral and target membranes, the DiD fluorophores diffuse away from each other, causing dequenching and allowing for the progression or inhibition of fusion to be measured in real time (**Supplementary Fig. 11**). Compared to NH_4Cl, an inhibitor of endosomal acidification[9], ezetimibe more potently inhibited HCVcc^{DiD} fusion, such that by 12 h after binding we measured only ~10% HCVcc^{DiD} dequenching in ezetimibe-treated cultures as compared to vehicle-treated controls (**Fig. 2i**). Analogously, antibody-mediated inhibition of both CD81 and NPC1L1 also reduced HCVcc^{DiD} fusion (**Fig. 2j**), indicating that the inhibition observed in ezetimibe-treated wells (**Fig. 2i**) was not drug specific. We also observed similar results using HCVcc^{DiD} alternatively purified by iodixanol density gradient centrifugation (**Supplementary Fig. 12a**,**b**).

As not all viral membrane–incorporated DiD is self-quenched, DiD can also serve as a fluorescent tag to monitor virions during cell entry[24]. Taking advantage of this, we performed fluorescence microscopy analysis of HCVcc^{DiD}-infected cultures and noted that although we observed little DiD on the surface of vehicle-treated cells, indicative of successful viral entry and fusion, we observed markedly more DiD on the surface of ezetimibe-treated cells (**Supplementary Fig. 12c**,**d**). Together with the DiD-fusion data, this indicates that inhibition of NPC1L1 prevents HCVcc cell entry at or before virion–host cell fusion.

Given that antibody-mediated blocking of only NPC1L1 LEL1 (**Fig. 1g**) reduced HCVcc infection, LEL1 has been shown to bind cholesterol[20,25] and infectious HCV particles are enriched in cholesterol[13,26], we next investigated whether the dependence of HCV cell entry on NPC1L1 might be related to the cholesterol contained within the HCV virions[13]. To address this hypothesis, we used viruses containing the E1/E2 glycoproteins derived from the HCV JFH-1 consensus clone but that differ in their virion-associated cholesterol content and assessed their relative dependence on NPC1L1. Specifically, we found that lentivirus particles pseudotyped with the JFH-1 HCV glycoproteins (HCVpp) contained 94% less cholesterol than the authentic JFH-1 HCVcc particles (HCVcc^{WT}). In contrast, cell culture–adapted HCVcc^{G451R} produced from a JFH-1 viral clone with a G451R point mutation in the viral E2 glycoprotein (HCVcc^{G451R}) contained ~50% more cholesterol than HCVcc^{WT} (**Fig. 3a**). These cholesterol profiles are consistent with

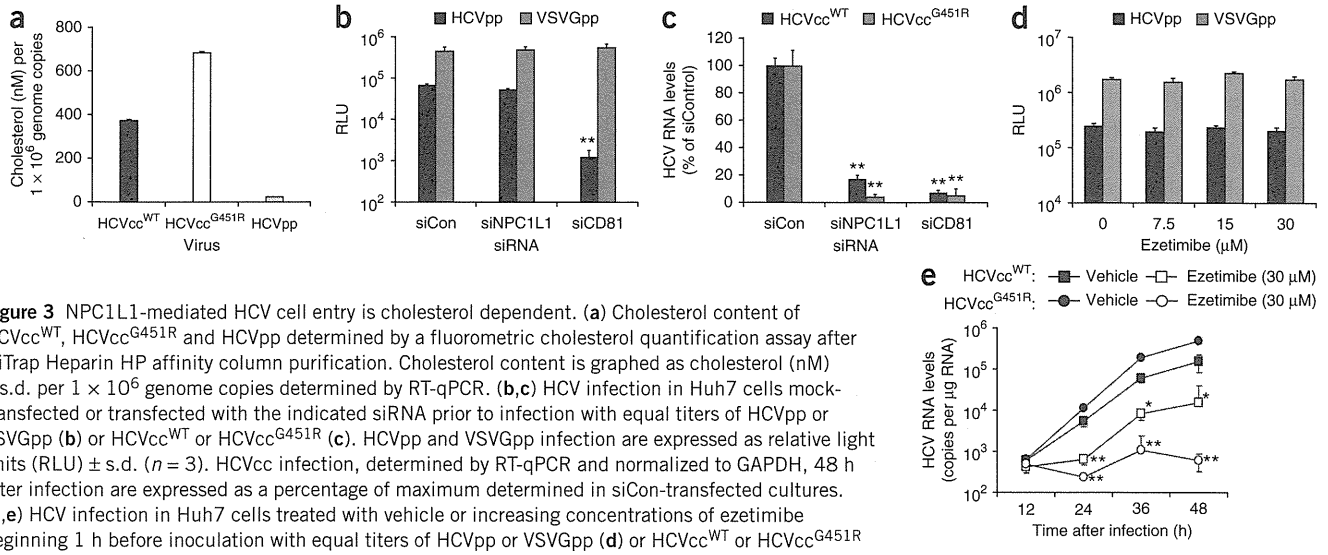

Figure 3 NPC1L1-mediated HCV cell entry is cholesterol dependent. (**a**) Cholesterol content of HCVcc^{WT}, HCVcc^{G451R} and HCVpp determined by a fluorometric cholesterol quantification assay after HiTrap Heparin HP affinity column purification. Cholesterol content is graphed as cholesterol (nM) ± s.d. per 1 × 10^6 genome copies determined by RT-qPCR. (**b**,**c**) HCV infection in Huh7 cells mock-transfected or transfected with the indicated siRNA prior to infection with equal titers of HCVpp or VSVGpp (**b**) or HCVcc^{WT} or HCVcc^{G451R} (**c**). HCVpp and VSVGpp infection are expressed as relative light units (RLU) ± s.d. (n = 3). HCVcc infection, determined by RT-qPCR and normalized to GAPDH, 48 h after infection are expressed as a percentage of maximum determined in siCon-transfected cultures. (**d**,**e**) HCV infection in Huh7 cells treated with vehicle or increasing concentrations of ezetimibe beginning 1 h before inoculation with equal titers of HCVpp or VSVGpp (**d**) or HCVcc^{WT} or HCVcc^{G451R} (**e**). HCVpp and VSVGpp infection are expressed as RLU ± s.d. (n = 3). HCVcc infection, determined by RT-qPCR and normalized to GAPDH, at the indicated times (h) after infection are expressed as mean HCV RNA copies per μg total cellular RNA ± s.d. *P < 0.05 and **P < 0.01 for RNA or RLU values relative to siCon-transfected or vehicle-treated cultures (one-way ANOVA and Tukey's post-hoc t test).

the fact that HCVpp is produced from 293T embryonal kidney cells, which do not produce cholesterol-associated lipoproteins[27], and are therefore compositionally distinct from HCVcc, whereas HCVcc^{G451R} has a narrower density range with a higher average mean density than the original JFH-1–derived HCVcc^{WT} (ref. 28). As expected, when CD81 was silenced, both HCVpp (**Fig. 3b**) and HCVcc^{G451R} (**Fig. 3c**) cell entry was reduced; however, when NPC1L1 was silenced or inhibited by ezetimibe, the cholesterol-scarce HCVpp showed NPC1L1-independent cell entry and insensitivity to ezetimibe inhibition (**Fig. 3b**,**d**). In contrast, the cholesterol-abundant HCVcc^{G451R} showed enhanced NPC1L1-dependent cell entry and hypersensitivity to ezetimibe-mediated inhibition (**Fig. 3c**,**e**). Together, these data reveal a correlation between the amount of virion-associated cholesterol and dependence on NPC1L1 for HCV cell entry.

Finally, to assess the involvement of NPC1L1 in HCV cell entry *in vivo*, we evaluated the ability of ezetimibe to inhibit infection of a genotype 1 clinical isolate in a hepatic xenorepopulation model of acute HCV infection[29]. Specifically, we repopulated urokinase-type plasminogen activator–severe combined immunodeficiency (uPA-SCID) mice with human hepatocytes and treated them via oral gavage with ezetimibe (10 mg per kg body weight per day) or diluent alone for a total of 3 weeks, with treatment beginning 2 weeks, 1 week or 2 d before challenge with HCV genotype 1b positive serum (**Fig. 4a**). Ezetimibe treatment delayed the establishment of HCV infection in mice pretreated for 2 weeks before infection (**Fig. 4b**, P = 0.0192), confirming the ability of this drug to inhibit HCV infection *in vivo*. However, when mice were pretreated for only 1 week before infection, ezetimibe was less effective at delaying infection (P = 0.062), and it was completely ineffective when treatment was initiated only 2 d before challenge or after infection had been established (data not shown). Specifically, 100% of the nine control diluent–treated mice were serum positive for HCV 1 week after challenge, whereas 71% (five out of seven) and 43% (three out of seven) of mice treated with ezetimibe for 2 weeks and 1 week before infection were HCV negative, respectively (**Fig. 4b**,**c**). Although the majority of ezetimibe-treated mice eventually became HCV positive, of the five mice in the 2-week ezetimibe pretreatment group that were HCV negative at week 1, two were completely protected, remaining HCV negative at weeks 2 and 3 after infection (and one mouse died during gavage) (**Supplementary Fig. 13**). Thus, similar to what was recently reported for another potential HCV entry inhibitor, erlotinib[30], ezetimibe was able to delay initial infection *in vivo*. Notably, since NPC1L1 is highly expressed on the apical surface of intestinal enterocytes[15,16], a considerable amount of orally administered ezetimibe initially binds to these cells following oral administration[31]. Thus it is plausible that development of alternate non-oral delivery or drug-targeting methods

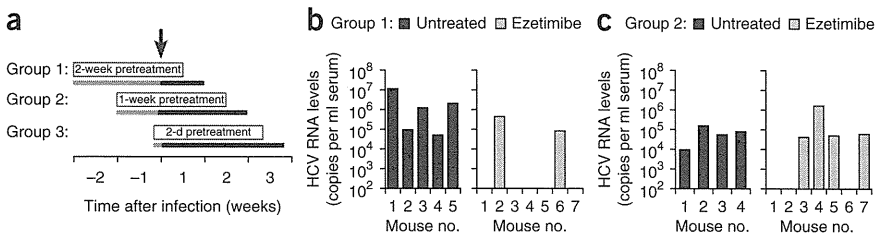

Figure 4 Ezetimibe delays the establishment of HCV infection in hepatic xenorepopulated mice. (**a**) Schematic diagram of an experiment in which uPA-SCID mice transplanted with human hepatocytes[35] were pretreated with diluent alone (n = 4 or 5) or ezetimibe (10 mg per kg body weight per day) (n = 7), via oral gavage, starting 2 weeks, 1 week or 2 d before infection (indicated by gray bars). The arrow indicates when the mice were intravenously inoculated on day 0 with HCV human serum containing 1.0 × 10^5 genome copies of HCV genotype 1b and the black bars indicate the time period post-HCV inoculation that treatments were continued. (**b**,**c**) HCV RNA levels (genome copies per milliliter of serum) 1 week after infection from mice pretreated for 2 weeks (**b**) or 1 week (**c**). The lower limit of HCV RNA detection is equal to 100 genomic copies per milliliter of serum. A two-tailed Fisher's exact test was performed to compare categorical variables. In all cases, P < 0.05 was used to reject the null hypothesis that the distribution of HCV-positive and HCV-negative mice between ezetimibe-treated and nine diluent-treated mice at specific weeks after infection were the same.

might improve transport of ezetimibe to hepatocytes and increase its anti-HCV efficacy. Nevertheless, our finding that ezetimibe can delay the establishment of HCV genotype 1 infection in mice confirms the involvement of NPC1L1 in HCV infection *in vivo* and highlights the therapeutic potential of further pursuing the refinement or development of anti-NPC1L1 therapies[32] for the treatment of HCV.

Here we have shown that NPC1L1 is an HCV cell entry factor that functions after binding, at or before fusion. These findings, together with the facts that NPC1L1 is a cellular cholesterol receptor, the HCV particle is enriched in cholesterol, and relative dependence on NPC1L1 is correlated with HCV particle cholesterol levels, support and expand upon previous reports suggesting that virion cholesterol is involved in HCV cell entry[13,14,26]. Whether NPC1L1 directly interacts with HCV or indirectly participates in HCV entry by removing virion-associated cholesterol to perhaps reveal protected viral glycoprotein binding sites or confer a required conformational change remains to be determined. Lastly, as NPC1L1 is expressed only on human and primate hepatocytes[33,34], this discovery additionally highlights NPC1L1 as a potential HCV tropism determinant, which may facilitate the future development of a small-animal model of HCV infection.

METHODS

Methods and any associated references are available in the online version of the paper at http://www.nature.com/naturemedicine/.

Note: Supplementary information is available on the Nature Medicine website.

ACKNOWLEDGMENTS

We thank T. Wakita (National Institute of Infectious Diseases, Japan) for JFH1-based plasmids, F. Chisari (The Scripps Research Institute) for Huh7 cells, J. Buhk (Copenhagen University Hospital Hepatitis C Program) for JFH-1–based intergenotypic HCV clones, Y. Ioannou (Mount Sinai School of Medicine) for the antibody (Bsn4052) against NPC1L1, D. Burton and M. Law (The Scripps Research Institute) for the antibody (C1) against the HCV glycoprotein E2 and C. Rice (The Rockefeller Institute) for the antibody (E910) against the HCV nonstructural protein NS5A. We would also like to thank P. Corcoran for outstanding technical assistance, H. Dahari for assistance with statistical analyses and T. Layden and S. Cotler for editing the manuscript. We also thank J. Graves of the University of Illinois at Chicago (UIC) Research Resources Center Flow Cytometry laboratory and K. Ma of the UIC Research Resources Center Confocal Microscopy laboratory for technical assistance. This work was supported by the US National Institutes of Health Public Health Service grants R01-AI070827 and R03-AI085226 (S.L.U.), the American Cancer Society Research Scholar Grant RSG-09-076-01 (S.L.U.), the UIC Center for Clinical and Translational Science NIH grant UL1RR029879, the UIC Council to Support Gastrointestinal and Liver Disease and a grant from the Ministry of Education, Culture, Sports, Science and Technology-Japan, Ministry of Health, Labour and Welfare-Japan (K.C.).

AUTHOR CONTRIBUTIONS

B.S. made the initial discovery. B.S. and S.L.U. designed the project, analyzed the results and wrote the manuscript. B.S., N.B., D.N.M., S.H., K.A.M. and X.Y. performed experimental work. B.S., S.L.U., M.I. and K.C. designed the hepatic xenorepopulation mouse experiments, and N.H. performed the *in vivo* studies. W.A.A. was involved in the initial conception of the project and provided valuable expertise.

COMPETING FINANCIAL INTERESTS

The authors declare competing financial interests: details accompany the full-text HTML version of the paper at http://www.nature.com/naturemedicine/.

Published online at http://www.nature.com/naturemedicine/.
Reprints and permissions information is available online at http://www.nature.com/reprints/index.html.

1. Uprichard, S.L. Hepatitis C virus experimental model systems and antiviral drug research. *Virol. Sin.* **25**, 227–245 (2010).
2. Gupta, E.K. & Ito, M.K. Ezetimibe: the first in a novel class of selective cholesterol-absorption inhibitors. *Heart Dis.* **4**, 399–409 (2002).
3. Garcia-Calvo, M. *et al.* The target of ezetimibe is Niemann-Pick C1-like 1 (NPC1L1). *Proc. Natl. Acad. Sci. USA* **102**, 8132–8137 (2005).
4. Pileri, P. *et al.* Binding of hepatitis C virus to CD81. *Science* **282**, 938–941 (1998).
5. Scarselli, E. *et al.* The human scavenger receptor class B type I is a novel candidate receptor for the hepatitis C virus. *EMBO J.* **21**, 5017–5025 (2002).
6. Evans, M.J. *et al.* Claudin-1 is a hepatitis C virus co-receptor required for a late step in entry. *Nature* **446**, 801–805 (2007).
7. Ploss, A. *et al.* Human occludin is a hepatitis C virus entry factor required for infection of mouse cells. *Nature* **457**, 882–886 (2009).
8. Liu, S. *et al.* Tight junction proteins claudin-1 and occludin control hepatitis C virus entry and are downregulated during infection to prevent superinfection. *J. Virol.* **83**, 2011–2014 (2009).
9. Tscherne, D.M. *et al.* Time- and temperature-dependent activation of hepatitis C virus for low-pH–triggered entry. *J. Virol.* **80**, 1734–1741 (2006).
10. Meertens, L., Bertaux, C. & Dragic, T. Hepatitis C virus entry requires a critical postinternalization step and delivery to early endosomes via clathrin-coated vesicles. *J. Virol.* **80**, 11571–11578 (2006).
11. Huang, H. *et al.* Hepatitis C virus production by human hepatocytes dependent on assembly and secretion of very low-density lipoproteins. *Proc. Natl. Acad. Sci. USA* **104**, 5848–5853 (2007).
12. Gastaminza, P. *et al.* Cellular determinants of hepatitis C virus assembly, maturation, degradation, and secretion. *J. Virol.* **82**, 2120–2129 (2008).
13. Aizaki, H. *et al.* Critical role of virion-associated cholesterol and sphingolipid in hepatitis C virus infection. *J. Virol.* **82**, 5715–5724 (2008).
14. Kapadia, S.B., Barth, H., Baumert, T., McKeating, J.A. & Chisari, F.V. Initiation of hepatitis C virus infection is dependent on cholesterol and cooperativity between CD81 and scavenger receptor B type I. *J. Virol.* **81**, 374–383 (2007).
15. Yu, L. The structure and function of Niemann-Pick C1–like 1 protein. *Curr. Opin. Lipidol.* **19**, 263–269 (2008).
16. Altmann, S.W. *et al.* Niemann-Pick C1 like 1 protein is critical for intestinal cholesterol absorption. *Science* **303**, 1201–1204 (2004).
17. Sané, A.T. *et al.* Localization and role of NPC1L1 in cholesterol absorption in human intestine. *J. Lipid Res.* **47**, 2112–2120 (2006).
18. Bays, H.E., Neff, D., Tomassini, J.E. & Tershakovec, A.M. Ezetimibe: cholesterol lowering and beyond. *Expert Rev. Cardiovasc. Ther.* **6**, 447–470 (2008).
19. Chang, T.Y. & Chang, C. Ezetimibe blocks internalization of the NPC1L1/cholesterol complex. *Cell Metab.* **7**, 469–471 (2008).
20. Weinglass, A.B. *et al.* Extracellular loop C of NPC1L1 is important for binding to ezetimibe. *Proc. Natl. Acad. Sci. USA* **105**, 11140–11145 (2008).
21. Gottwein, J.M. *et al.* Development and characterization of hepatitis C virus genotype 1–7 cell culture systems: role of CD81 and scavenger receptor class B type I and effect of antiviral drugs. *Hepatology* **49**, 364–377 (2009).
22. Grove, J. *et al.* Scavenger receptor BI and BII expression levels modulate hepatitis C virus infectivity. *J. Virol.* **81**, 3162–3169 (2007).
23. Zaitseva, E., Yang, S.T., Melikov, K., Pourmal, S. & Chernomordik, L.V. Dengue virus ensures its fusion in late endosomes using compartment-specific lipids. *PLoS Pathog.* **6**, e1001131 (2010).
24. Coller, K.E. *et al.* RNA interference and single particle tracking analysis of hepatitis C virus endocytosis. *PLoS Pathog.* **5**, e1000702 (2009).
25. Zhang, J.H. *et al.* The N-terminal domain of NPC1L1 protein binds cholesterol and plays essential roles in cholesterol uptake. *J. Biol. Chem.* **286**, 25088–25097 (2011).
26. Yamamoto, M. *et al.* Structural requirements of virion-associated cholesterol for infectivity, buoyant density and apolipoprotein association of hepatitis C virus. *J. Gen. Virol.* **92**, 2082–2087 (2011).
27. Farquhar, M.J. & McKeating, J.A. Primary hepatocytes as targets for hepatitis C virus replication. *J. Viral Hepat.* **15**, 849–854 (2008).
28. Zhong, J. *et al.* Persistent hepatitis C virus infection in vitro: coevolution of virus and host. *J. Virol.* **80**, 11082–11093 (2006).
29. Kneteman, N.M. & Toso, C. *In vivo* study of HCV in mice with chimeric human livers. *Methods Mol. Biol.* **510**, 383–399 (2009).
30. Lupberger, J. *et al.* EGFR and EphA2 are host factors for hepatitis C virus entry and possible targets for antiviral therapy. *Nat. Med.* **17**, 589–595 (2011).
31. Sweeney, M.E. & Johnson, R.R. Ezetimibe: an update on the mechanism of action, pharmacokinetics and recent clinical trials. *Expert Opin. Drug Metab. Toxicol.* **3**, 441–450 (2007).
32. Betters, J.L. & Yu, L. Transporters as drug targets: discovery and development of NPC1L1 inhibitors. *Clin. Pharmacol. Ther.* **87**, 117–121 (2010).
33. Davies, J.P., Scott, C., Oishi, K., Liapis, A. & Ioannou, Y.A. Inactivation of NPC1L1 causes multiple lipid transport defects and protects against diet-induced hypercholesterolemia. *J. Biol. Chem.* **280**, 12710–12720 (2005).
34. Davis, H.R. Jr. *et al.* Niemann-Pick C1 like 1 (NPC1L1) is the intestinal phytosterol and cholesterol transporter and a key modulator of whole-body cholesterol homeostasis. *J. Biol. Chem.* **279**, 33586–33592 (2004).
35. Matsumura, T. *et al.* Amphipathic DNA polymers inhibit hepatitis C virus infection by blocking viral entry. *Gastroenterology* **137**, 673–681 (2009).

ONLINE METHODS

HCVcc. Plasmids containing the full-length HCV JFH-1 genome (pJFH1)[36], full-length HCV JFH-1 genome with a G451R mutation in the E2 glycoprotein (pJFH-1^{G451R})[37] and the eight intergenotypic clones (described in ref. 21) were XbaI linearized and transcribed using MEGAscript T7 (Ambion), and 10 μg *in vitro*–transcribed RNA was electroporated (BioRad) into Huh7 cells[38]. We generated HCVcc viral stocks by infecting naive Huh7 cells at an MOI of 0.01 FFU per cell with medium from Huh7 cells electroporated with *in vitro*–transcribed RNA from pJFH-1–based vectors, as previously described[38].

Treatments and analysis. Huh7 cultures were established as previously described[38]. We performed RNA silencing experiments by reverse transfection (Lipofectamine RNAiMAX, Invitrogen) of siRNAs into Huh7 cells. Transfected cells were infected with equal titers of HCVpp or VSVGpp or HCVcc at an MOI of 0.05 FFU per cell) at the indicated times after transfection (**Fig. 1c–e**). For antibody experiments, we treated cells with 36 μg ml^{-1} of antibody before and during infection with HCVcc at an MOI of 0.05 FFU per cell. For ezetimibe inhibition experiments, cells were vehicle-treated or treated with increasing concentrations of ezetimibe (Sequoia Research Products) before infection, during the time of virus inoculation and/or after virus inoculation with HCVcc at an MOI of 0.1–1.0 FFU per cell. The ezetimibe concentrations of 3.125–30 μM (that is, 1.5–12.28 μg per ml culture medium) used in this study are consistent with previously published reports[19,20,39] and are additionally in line with patient daily intake concentrations of 10 mg d^{-1} (that is, 2.0–3.3 μg per ml of serum). For RT-qPCR analysis, we isolated total cellular RNA from triplicate culture wells after infection or transfection. For HCV E2–positive foci analysis, we fixed infected cells with 4% (wt/vol) paraformaldehyde 72 h after infection, and immunocytochemical staining for HCV E2 was performed. See **Supplementary Methods** for further details.

HCV infection in chimeric mice. All mouse studies were conducted with protocols approved by the Ethics Review Committee for Animal Experimentation of the Graduate School of Biomedical Sciences, Hiroshima University. Male uPA-SCID mice transplanted with human hepatocytes (BD Biosciences[35]) were purchased from PhenixBio[40]. Mice were treated daily with 10 mg per kg body weight ezetimibe via oral gavage of a 0.02 mg ml^{-1} solution of ezetimibe resuspended in corn oil (100 μl 20g^{-1}) for a total of 3 weeks, with treatment initiation beginning 2 weeks, 1 week or 2 d before infection[16]. Control mice were treated via oral gavage with corn oil alone (100 μl per 20 g body weight). A total of four to seven mice were included in each group. On day 0, we intravenously inoculated mice with serum from HCV-infected humans containing 1.0×10^5 copies of HCV genotype 1b. Mouse serum samples were obtained for HCV RNA or human albumin determination by RT-qPCR and Alb-II Kit (Eiken Chemical), respectively.

Statistical analyses. Data are presented as the means ± s.d. We determined significant differences by one-way ANOVA followed by Tukey's post-hoc *t* test (GraphPad Prism software). To compare categorical variables we used a two-tailed Fisher's exact test (SPSS). In all cases, a P value <0.05 was considered statistically significant.

Additional methods. Detailed methodology is described in the **Supplementary Methods**.

36. Wakita, T. *et al.* Production of infectious hepatitis C virus in tissue culture from a cloned viral genome. *Nat. Med.* **11**, 791–796 (2005).
37. Sabahi, A. *et al.* The rate of hepatitis C virus infection initiation *in vitro* is directly related to particle density. *Virology* **407**, 110–119 (2010).
38. Yu, X. & Uprichard, S.L. Cell-based hepatitis C virus infection fluorescence resonance energy transfer (FRET) assay for antiviral compound screening. *Curr. Protoc. Microbiol.* **18**, 17.5.1–17.5.27 (2010).
39. Ge, L. *et al.* The cholesterol absorption inhibitor ezetimibe acts by blocking the sterol-induced internalization of NPC1L1. *Cell Metab.* **7**, 508–519 (2008).
40. Tateno, C. *et al.* Near completely humanized liver in mice shows human-type metabolic responses to drugs. *Am. J. Pathol.* **165**, 901–912 (2004).

doi:10.1038/nm.2581

J Gastroenterol (2012) 47:834–844
DOI 10.1007/s00535-012-0550-y

ORIGINAL ARTICLE—LIVER, PANCREAS, AND BILIARY TRACT

IL28B polymorphism is associated with fatty change in the liver of chronic hepatitis C patients

Mayu Ohnishi · Masataka Tsuge · Tomohiko Kohno · Yizhou Zhang · Hiromi Abe · Hideyuki Hyogo · Yuki Kimura · Daiki Miki · Nobuhiko Hiraga · Michio Imamura · Shoichi Takahashi · Hidenori Ochi · C. Nelson Hayes · Shinji Tanaka · Koji Arihiro · Kazuaki Chayama

Received: 17 November 2011 / Accepted: 18 January 2012 / Published online: 18 February 2012

Abstract
Background Several single nucleotide polymorphisms (SNPs) within the *interleukin 28B* (*IL28B*) locus are associated with sustained viral response in chronic hepatitis C (HCV) patients who were treated with pegylated interferon (PEG-IFN) plus ribavirin (RBV) combination therapy. Recently, an association between γ-GTP level and IL28B genotype was identified. In this study, the relationship between IL28B genotype and liver steatosis was analyzed.
Methods One hundred fifty-three patients who underwent liver biopsy before PEG-IFN plus RBV combination therapy were enrolled. The level of liver steatosis was measured using a BIOREVO BZ-9000 microscope, and the proportion of fatty change and clear cell change were calculated using Dynamic cell count BZ-H1C software. IL28B SNP genotype (rs8099917) was determined using the Invader Assay.
Results Vesicular change was significantly associated with body mass index (BMI), HCV RNA titer, serum aspartate aminotransferase, γ-GTP, IL28B genotype and liver fibrosis level ($P < 0.05$). Clear cell change was significantly associated with serum aspartate aminotransferase, γ-GTP and IL28B genotype by univariate logistic regression analysis ($P < 0.05$). Under multiple logistic regression, IL28B genotype ($OR_{adj} = 8.158$; 95% CI 2.412–27.589), liver fibrosis ($OR_{adj} = 2.541$; 95% CI 1.040–6.207) and BMI ($OR_{adj} = 1.147$; 95% CI 1.011–1.301) were significant independent factors for vesicular change and IL28B genotype ($OR_{adj} = 3.000$; 95% CI 1.282–7.019) for clear cell change.
Conclusion In this study, a new quantitative method to objectively evaluate hepatic steatosis was described. IL28B genotypes were significantly associated with both vesicular and clear cell changes of livers in chronic hepatitis C patients.

Keywords HCV · Core substitution · IL28B · Fatty change · SNP

Abbreviations

HCV	Hepatitis C virus
IFN	Interferon

M. Ohnishi · M. Tsuge · T. Kohno · Y. Zhang · H. Abe · H. Hyogo · Y. Kimura · D. Miki · N. Hiraga · M. Imamura · S. Takahashi · H. Ochi · C. N. Hayes · S. Tanaka · K. Chayama
Programs for Biomedical Research, Division of Frontier Medical Science, Department of Gastroenterology and Metabolism, Graduate School of Biomedical Sciences, Hiroshima University, Hiroshima, Japan

M. Ohnishi · M. Tsuge · T. Kohno · Y. Zhang · H. Abe · H. Hyogo · Y. Kimura · D. Miki · N. Hiraga · M. Imamura · S. Takahashi · H. Ochi · C. N. Hayes · K. Chayama
Liver Research Project Center, Hiroshima University, Hiroshima, Japan

M. Tsuge
Natural Science Center for Basic Research and Development, Hiroshima University, Hiroshima, Japan

D. Miki · H. Ochi · K. Chayama
Laboratory for Digestive Diseases, Center for Genomic Medicine, RIKEN, Hiroshima, Japan

K. Arihiro
Department of Pathology, Hiroshima University Hospital, Hiroshima, Japan

K. Chayama (✉)
Programs for Biomedical Research, Division of Frontier Medical Science, Department of Medical and Molecular Science, Graduate School of Biomedical Sciences, Hiroshima University, 1-2-3 Kasumi, Minami-ku, Hiroshima, Japan
e-mail: chayama@hiroshima-u.ac.jp

PEG-IFN	Pegylated interferon
RBV	Ribavirin
ISDR	IFN-sensitivity determining region
IL28	Interleukin 28
SNP	Single nucleotide polymorphism
BMI	Body mass index
γ-GTP	Gamma glutamyl transpeptidase
aa	Amino acid
HOMA-IR	Homeostasis model assessment of insulin resistance

Background

Hepatitis C virus (HCV) is one of the most serious global health problems, affecting more than 170 million people worldwide [1–3]. Chronic HCV infection leads to the development of chronic hepatitis, cirrhosis and hepatocellular carcinoma (HCC) [4–8]. To attempt to eradicate the virus and prevent the development of advanced liver diseases and HCC, interferon is administered to chronic hepatitis C patients, with success in a subset of patients in which marked biochemical and histological improvements can be obtained [9, 10]. However, patients with a high virus titer and those who are infected with genotype 1b, which is the major genotype affecting about 70% of Japanese patients, show poor response to interferon monotherapy. Less than 20% of patients treated with interferon monotherapy show sustained virological response [11–14]. With the advent of pegylated interferon (PEG-IFN) and ribavirin (RBV) combination therapy, the eradication rate of the virus has improved. However, the eradication rate of genotype 1b with high viral load still remains only 40–50% [15–17].

Several viral and host factors have been identified that are predictive of the outcome of PEG-IFN plus RBV combination therapy. HCV genotype, HCV RNA level and HCV amino acid (aa) substitutions in the core region and the interferon-sensitivity determining region (ISDR; aa positions 237–276 of the NS5A region) have been reported as viral factors for achieving sustained viral response. On the other hand, host factors, such as patient age, gender, liver fibrosis stage, liver steatosis and homeostasis model assessment of insulin resistance (HOMA-IR), are also known to be associated with IFN response. Okanoue et al. demonstrated that the frequency of liver steatosis and HOMA-IR were significantly lower in patients who achieved sustained virological response than those who did not [18–23].

Recently, genome-wide association studies (GWAS) have examined the association between human genetic variation and the response to IFN treatment, and several common polymorphisms in the interleukin 28B (IL28B) locus were found to predict successful HCV clearance with IFN therapy [24–27]. IL28B single nucleotide polymorphisms (SNPs) (rs12979860, rs8099917, and rs12980275) are strongly associated with sustained virological response in patients who undergo PEG-IFN plus RBV combination therapy. In a recent study, the serum γ-GTP level was also found to be associated with the IL28B SNP (rs8099917) genotype in patients infected with HCV genotype 1b [28]. Serum γ-GTP levels were significantly lower in patients homozygous for the major allele (TT) than in patients with the minor allele (GG or GT) [28]. On the other hand, the serum γ-GTP level is well known to be related to liver steatosis; therefore, it was hypothesized that the levels of liver steatosis may be associated with the IL28B genotype. In the present study, a quantitative method to evaluate fatty change was established, and the association between fatty change and host or viral factors was analyzed.

Patients and methods

Patients

Three hundred fifty-three adult Japanese patients infected with HCV genotype 1b provided written informed consent to participate in the present study at Hiroshima University Hospital, Hiroshima, Japan. Among these patients, 153 who underwent liver biopsy or hepatic resection from December 2001 to August 2009 before commencing antiviral therapy were selected for the study based on the following exclusion criteria: (1) not co-infected with other viruses, such as human immunodeficiency virus or hepatitis B virus; (2) no other liver diseases such as hemochromatosis, auto-immune hepatitis or decompensated cirrhosis; (3) no co-existing diseases such as de-compensated renal disease, pre-existing psychiatric disease, seizure disorders, cardiovascular disease, hemophilia, autoimmune diseases or post-transplantation. The experimental protocol conformed to the ethical guidelines of the 1975 Declaration of Helsinki and was approved by the Hiroshima University Hospital ethics committee. Written informed consent was obtained from each patient. Patients whose ethanol intake was more than 20 g/day were defined as alcoholic [29, 30]. Baseline characteristics of the 153 patients are shown in Table 1.

Evaluation of liver steatosis

Liver tissues with hematoxylin–eosin stain were used in this study. Liver fibrosis and activity stages were diagnosed by a pathologist at Hiroshima University Hospital according to the criteria of Desmet et al. [31]. The level of liver steatosis was measured using a BIOREVO BZ-9000 microscope (Keyence, Osaka, Japan), and the proportion of

Table 1 Clinical backgrounds of patients

Characteristics	
Age (years)[a]	60 (15–76)
Gender (M:F)	83:70
BMI (kg m^{-2})[a]	22.7 (16.2–39.4)
Alcohol (+:−)	47:103
Laboratory data	
Platelet count ($\times 10^3$ μl^{-1})[a]	99 (23–759)
Prothrombin activity (%)[a]	99 (12–166)
Total bilirubin (mg dl^{-1})[a]	0.7 (0.4–14.7)
Aspartate aminotransferase (IU l^{-1})[a]	46 (14–2617)
Alanine aminotransferase (IU l^{-1})[a]	51 (2–2707)
Lactate dehydrogenase (IU l^{-1})[a]	202 (43–899)
Gamma glutamyl transpeptidase (IU l^{-1})[a]	43 (12–295)
Albumin (g dl^{-1})[a]	4.3 (2.9–5.3)
Total cholesterol (mg dl^{-1})[a]	174 (100–312)
Triglycerides (mg dl^{-1})[a]	100 (33–2466)
Glucose (mg dl^{-1})[a]	101 (68–334)
HCV RNA (log IU ml^{-1})[a]	6.3 (4.2–7.9)
Core 70 (wild:mutant)	77:39
Core 91 (wild:mutant)	54:62
ISDR (0:≥1)	38:76
IL28B (TT:TG:GG)	116:33:4
Liver histology	
Fibrosis (F0–1:F2–3)	42:111
Inflammatory activity (A0–1:A2–3)	59:94

[a] Median (range)

fatty change was calculated using Dynamic cell count BZ-H1C software (Keyence). The average of the observed area was 3.03 mm^2 (0.74–6.77 mm^2). The distribution of brightness values in liver tissue images was evaluated using a brightness distribution histogram as shown in Fig. 1a. The brightness was divided into 256 gradation sequences. Regions with a brightness value over 60% between minimum and maximum brightness were considered to represent fatty change areas in the liver tissue. The area of interest was calculated, and <5 μm^2 of the extracted areas were excluded as noise as determined by particle elimination technology (Dynamic cell count BZ-H1C software) (Fig. 1b). The remaining highlighted noise, including glycogen nuclei and vascular spaces, was excluded as much as possible by visual observation. After two exclusion steps, the remaining noise spaces were sufficiently narrow (far <5% of total fatty changed spaces) that they could be considered negligible. The observed area of the sample was also calculated with BZ-H1C software (Fig. 1c). All threshold values of vesicular change or clear cell change ratio were defined based on the approximate median values of each change.

Determination of amino acid sequences in the HCV core region and ISDR

HCV RNA was extracted from 100 µl of stored serum samples by SepaGene RV-R (Sanko Junyaku Co., Ltd, Tokyo, Japan), dissolved in 20 µl of H_2O and converted to cDNA by RT with random primers and MMLV reverse transcriptase (Takara Shuzo, Tokyo, Japan). The cDNA was then amplified by nested PCR to determine the nucleotide sequences in the HCV core region. The PCR protocol was as follows: initial denaturation at 95°C for 5 min, 35 cycles of denaturation for 30 s at 94°C, annealing of primers for 1 min at 57°C and extension for 1 min at 72°C, followed by a final extension at 72°C for 7 min. The primers for the first round PCR were cc11 (forward, 5′-GCC ATA GTG GTC TGC GGA AC-3′) and e14 (reverse, 5′-GGA GCA GTC CTT CGT GAC ATG-3′), and the primers for the second-round PCR were cc9 (forward, 5′-GCT AGC CGA GTA GTG TT-3′) and e14 (reverse), as described previously [19, 21, 32, 33]. To determine the nucleotide sequences of the HCV ISDR region, we also performed nested PCR with the same protocol as in the HCV core region. The primers used were IM11 (forward, 5′-TTC CAC TAC GTG ACG GGC AT-3′) and 5A02KI (reverse, 5′-CCC GTC CAT GTG TAG GAC AT-3′) for the first round PCR, and 5A05KI (forward, 5′-GGG TCA CAG CTC CCA TGT GAG CC -3′), and IM10 (reverse, 5′-GAG GGT TGT AAT CCG GGC GTG C-3′) for the second round PCR. After amplification, the final PCR products were separated in 2% agarose gel and purified with the QIAquick gel extraction kit (QIAGEN GmbH, Hilden, Germany). Sequence analysis was performed by ABI Prism 3100 Avant Genetic Analyzer (Applied Biosystems, Foster City, CA, USA). Amino acid sequences were compared with the genotype 1b HCV-J reference sequence (Gene Bank accession no. D90208) [34]. Arginine and leucine were considered wild type for amino acids 70 and 91, respectively, and the most frequent amino acid substitutions were glutamine or histidine at aa 70 and methionine at aa 91.

Determination of genotype in IL28B

In Asian populations, the genotype of rs8099917, a SNP within the *IL28B* locus, has been reported to be strongly correlated to nearby SNPs rs12979860 and rs12980275 because of strong linkage disequilibrium [35]. In this study, rs8099917 was used to represent the genotype of the *IL28B* SNP. Genotypes of rs8099917 were determined using TaqMan® Pre-Designed SNP Genotyping Assays as described previously [28].

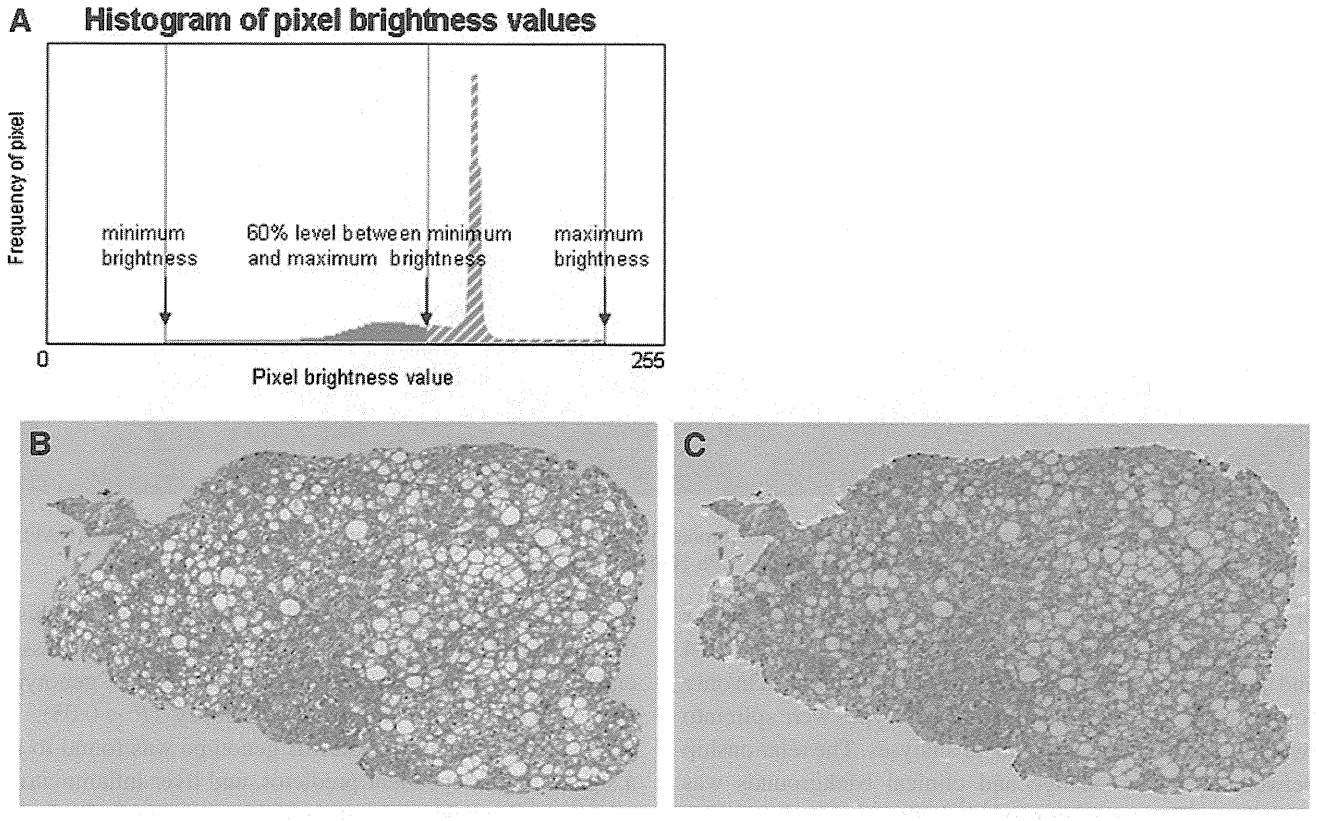

Fig. 1 Evaluation of fatty change in liver tissue. **a** The distribution of brightness in liver tissue images was represented with a brightness distribution histogram using BZ-H1C software. The relative cumulative frequency of pixels with brightness values over 60% between minimum and maximum brightness was interpreted as the proportion of fatty change in the liver tissue. **b** The area of the fatty change is depicted in *yellow*. **c** The area inside the *yellow line* is defined as the observed area (color figure online)

Statistical analysis

In univariate analysis, the clinical backgrounds of the patients in the two groups were compared, and differences were assessed by chi-square test with Yate's correction for categorical variables and by Mann–Whitney *U* test for continuous variables. All thresholds were determined based on median values. All *P* values <0.05 by two-tailed test were considered statistically significant. To analyze the association between clinical characteristics and fatty change, multivariate logistic regression analysis was performed. To identify significant independent predictive factors, variables with statistical significance ($P < 0.05$) or marginal significance ($P < 0.10$) in univariate analysis were used as the starting model for forward stepwise logistic regression model using the likelihood ratio test. Statistical analyses were performed using SPSS 17.0 (SPSS Inc., Chicago, IL, USA).

Results

Patterns of histological change in the liver

Comparing the liver tissues between chronic hepatitis C and non-alcoholic fatty liver disease, we identified two different histological change patterns. As shown in Fig. 2, histological change in patients with non-alcoholic fatty liver disease consisted mainly of vesicular change (Fig. 2a), but histological change in the chronic hepatitis C patients consisted of both vesicular change and clear cell change (Fig. 2b), suggesting that clear cell change was the distinguishing change in chronic hepatitis C. Accordingly, we further analyzed liver specimens from patients with these diseases to determine the best criteria to distinguish clear cell change areas from vesicular change areas. Most of the vesicular change areas were found to be more than 200 μm^2 (data not shown). Therefore, we defined areas with <200 μm^2 of fatty change as areas of clear cell change (Fig. 3). Although narrow noise spaces (<200 μm^2), including small vacuoles or hepatocyte nucleus, remained after these automatic steps, the remaining noise spaces were then excluded as much as possible by visual observation. As shown in Fig. 4, the distribution of vesicular change was associated with clear cell change.

Association between vesicular change and clinical background

To analyze the relationship between fatty change and clinical background, we compiled the clinical backgrounds

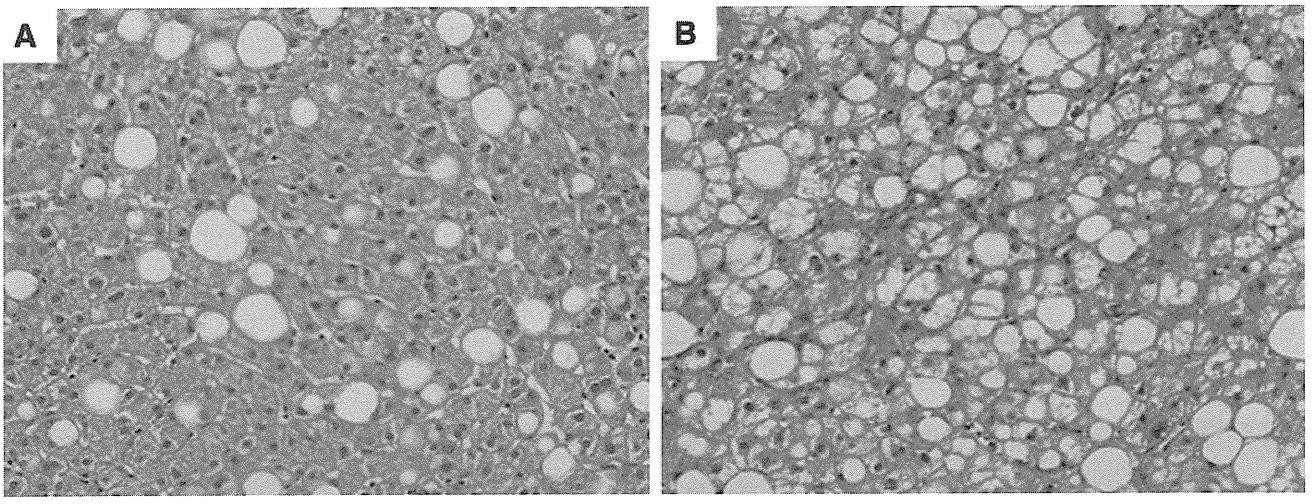

Fig. 2 Different fatty change patterns between NAFLD and chronic hepatitis C. The fatty change pattern was compared between NAFLD (**a**) and chronic hepatitis C (**b**). The liver tissues were stained with H&E

of 153 participating patients (Table 1). Because the minor allele frequency of the IL28B rs8099917 SNP was only 0.14 and the IL28B rs8099917 GG genotype was observed in only four patients, the IL28B rs8099917 genotypes were split into two groups (TT vs. TG/GG) in all analyses. The relationship between vesicular change and clinical backgrounds was examined. The proportion of vesicular change (vesicular change ratio) was defined as the ratio of the area of vesicular change and the observed area (= area of vesicular change/observed area). As shown in Table 2, in univariate analysis the greater vesicular change ratio was significantly associated with γ-GTP, *IL28B* genotype, aspartate aminotransferase, body mass index (BMI), liver fibrosis stage and HCV RNA at the point of liver biopsy ($P < 0.05$). The association between IL28B genotype and vesicular change was examined using multivariate analysis, and *IL28B* genotype, liver fibrosis stage and BMI were retained in the final model (Table 2). These results indicate that the vesicular change was not only associated with *IL28B* genotype, but also associated with BMI. To confirm the association between *IL28B* genotypes and vesicular change, multiple regression analysis was also performed using continuous values. *IL28B* genotype, HCV RNA titer and liver fibrosis stage were identified as independent factors for vesicular change ($P = 0.003$, $P = 0.022$, $P = 0.047$, respectively).

Association between clear cell change and clinical background

Next, the relationship between clear cell change and clinical background was analyzed. The proportion of clear cell change (clear cell change ratio) was defined as the ratio of the area of the clear cell change and the observed area (= area of clear cell change/observed area). We divided the study subjects into two groups according to the clear cell change ratio. As shown in Table 3, in univariate analysis the greater clear cell change ratio was significantly associated with aspartate aminotransferase, IL28B genotype and γ-GTP at the point of liver biopsy ($P < 0.05$). In multivariate analysis, the IL28B genotype was found to be a significant independent predictor, and liver inflammatory activity and gender were marginally associated (Table 3). By using continuous values in multiple regression, the *IL28B* genotype was also identified as an independent factor for clear cell change ($P < 0.001$). These results suggest that the *IL28B* genotype is significantly associated with clear cell change in livers of chronic hepatitis C patients.

The association between fatty degeneration and IL28B genotype in the non-obese group

To analyze the association between fatty change and IL28B genotype, the study subjects were divided into two groups. Thirty-six patients whose BMI was more than 25 kg m^{-2} were assigned to the obese group, and the other 114 patients were assigned to the non-obese group. In the obese group, no association between fatty change and IL28B genotype was observed (Table 4). On the other hand, each measure of fatty change (vesicular change, and clear cell change) was significantly associated with IL28B genotype in the non-obese group ($P = 0.001$, $P = 0.009$, respectively, Table 4).

Discussion

It is generally difficult to compare evaluations of liver fatty change because such studies depend on the respective assessments of individual pathologists [36, 37]. In the

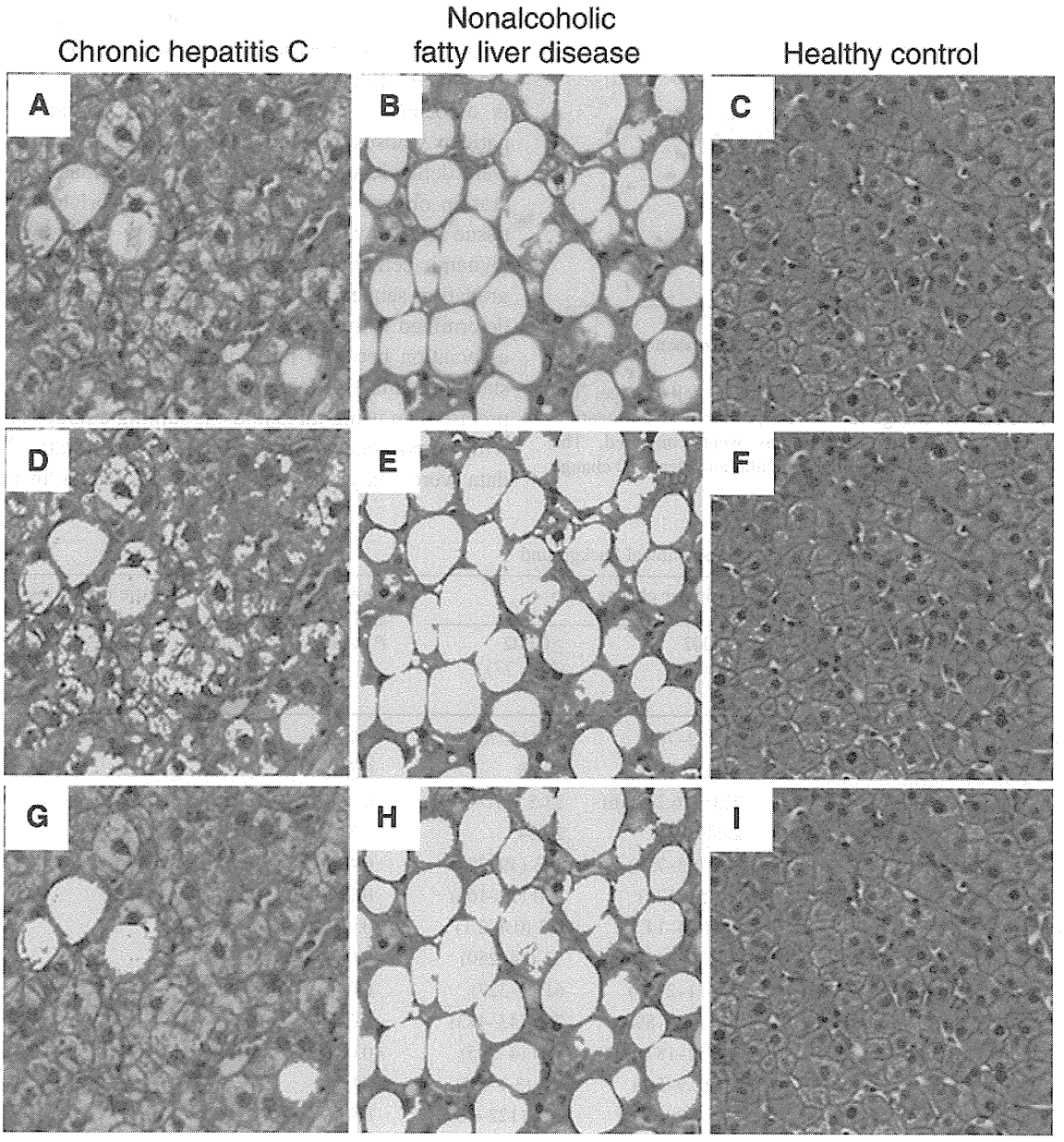

Fig. 3 Discrimination between vesicular and clear cell change. The evaluation results of three cases are shown. The *upper panels* are H&E staining of liver specimen from NAFLD (**a**), chronic hepatitis C (**b**) and a healthy control (**c**). In the *middle panels*, the fatty change area is depicted in *yellow* (**d–f**). In the *lower panels*, the vesicular change area is preferentially depicted with *yellow* using a criteria of $<200\ \mu m^2$ of fatty change (**g–i**) (color figure online)

present study, we established criteria by which the degree of liver fatty change can be evaluated objectively. It is well known that the proportions of fatty change differ by location in liver tissues obtained by liver biopsy or operation. For quantitative evaluation of fatty change, an efficient algorithm was devised using the BIOREVO BZ-9000 microscope and Dynamic cell count BZ-H1C software. Using this method, fatty changes were analyzed in whole tissue specimens in chronic hepatitis C patients. With this algorithm, it was possible to evaluate fatty changes of whole tissues in the slides and obtain the same results by different operators. Furthermore, vesicular changes and clear cell changes could be evaluated separately by the distribution of brightness in liver tissues.

The main limitation of this study is that some selection biases and confounders such as alcohol consumption and the definition of fatty degeneration might affect the internal validity of the study. The study subjects were selected based on a history of liver biopsy or liver resection and infection with HCV genotype 1b. As levels of steatosis have been shown to differ among HCV genotypes, the present study was restricted to HCV genotype 1b, which

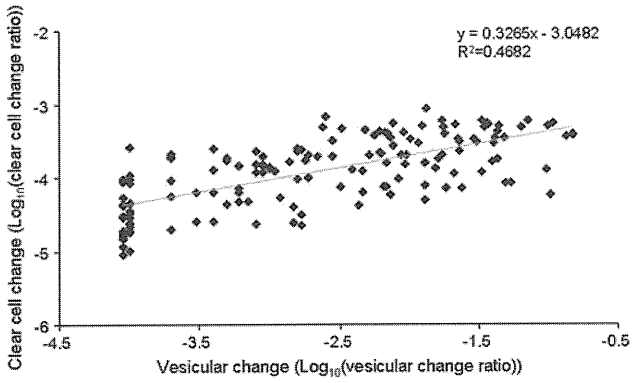

Fig. 4 Association between vesicular and clear cell change. The vesicular and clear cell change ratios were performed with logarithmic transformation, and the distributions were compared. The association between the distribution of vesicular and clear cell change are shown by a scatter diagram

accounts for more than 70% of chronic hepatitis C cases in Japan and is the best studied with respect to IL28B polymorphisms. Because ethanol intake of more than 20 g/day is associated with progressive liver damage [29, 30], patients whose daily alcohol intake exceeded this threshold were defined as alcohol positive. To evaluate fatty degeneration objectively, the distribution of brightness in liver tissue images was used. The brightness was calculated with Dynamic cell count BZ-H1C software and divided into 256 gradation sequences, and the fatty degeneration area was determined with the fixed brightness range. To evaluate the association between fatty degeneration and other factors, statistical analysis using continuous values may be more precise than using thresholds, assuming a large sample size with homoskedastic, normally distributed data. When the data were analyzed using continuous values in univariate

Table 2 Association between vesicular change and clinical background

	Vesicular change ratio		Univariate analysis	Multiple logistic regression analysis		
	<0.002 ($N = 76$)	≥0.002 ($N = 77$)	*P* value	*P* value	Adjusted odds ratio	95% CI
Age (years)[a]	60 (22–76)	61 (15–76)	0.774			
Gender (M:F)	44:32	39:38	0.368**			
BMI (kg m^{-2})[a]	22.0 (16.2–30.6)	23.5 (17.7–39.4)	0.009	0.033	1.147	1.011–1.301
Alcohol (+:−)	26:49	21:54	0.379**			
Platelet count ($\times 10^3$ μl^{-1})[a]	144 (23–759)	143 (49–327)	0.436			
Prothrombin activity (%)[a]	99 (56–124)	100 (12–166)	0.727			
Total bilirubin (mg dl^{-1})[a]	0.7 (0.4–14.7)	0.7 (0.4–2.1)	0.922			
Aspartate aminotransferase (IU l^{-1})[a]	42 (20–2617)	53 (14–250)	0.008	0.317		
Alanine aminotransferase (IU l^{-1})[a]	48 (11–2707)	61 (2–327)	0.093	0.318		
Lactate dehydrogenase (IU l^{-1})[a]	197 (129–899)	204 (43–473)	0.286			
Gamma glutamyl transpeptidase (IU l^{-1})[a]	34 (12–187)	55 (14–295)	<0.001	0.110		
Albumin (g dl^{-1})[a]	4.4 (2.9–5.3)	4.2 (3.1–5.1)	0.069			
Total cholesterol (mg dl^{-1})[a]	174 (100–312)	174 (122–263)	0.975			
Triglycerides (mg dl^{-1})[a]	97 (33–339)	113 (35–2466)	0.141			
Glucose (mg dl^{-1})[a]	98 (68–334)	103 (70–237)	0.533			
HCV RNA (log IU ml^{-1})[a]	6.4 (4.2–7.9)	6.2 (4.2–7.5)	0.031	0.068		
Core 70 (wild:mutant)	37:12	40:27	0.075**	0.230		
Core 91 (wild:mutant)	21:28	33:34	0.495**			
ISDR (0:≥1)	15:33	23:43	0.687**			
IL28B (TT:TG or GG)	65:11	51:26	0.005**	0.001	8.158[b]	2.412–27.589
Fibrosis (F0–1:F2–3)	36:40	23:54	0.026**	0.041	2.541[c]	1.040–6.207
Inflammatory activity (A0–1:A2–3)	24:51	17:60	0.168**			

Univariate analysis was performed with Mann–Whitney *U* test and **chi-square test

Multiple logistic regression analysis was performed using variables that were significant ($P < 0.05$) or marginally significant ($P < 0.10$) in univariate analysis

[a] Median (range)

[b] IL28B genotypes were coded as 0 or 1 depending on whether the subject carried the minor allele

[c] Fibrosis was coded as 0 for patients with mild fibrosis (F0–1) and 1 for patients with severe fibrosis (F2–3)

Table 3 Association between clear cell change and clinical background

	Clear cell change ratio		Univariate analysis	Multiple logistic regression analysis		
	<0.03 ($N = 77$)	≥0.03 ($N = 76$)	P value	P value	Adjusted odds ratio	95% CI
Age (years)[a]	60 (22–76)	61 (15–76)	0.408			
Gender (M:F)	47:29	36:41	0.061**	0.057		
BMI (kg m^{-2})[a]	23.0 (16.2–32.3)	22.7 (17.6–39.4)	0.477			
Alcohol (+:−)	27:47	20:56	0.179**			
Platelet count ($\times 10^3$ μl^{-1})[a]	152 (23–759)	131 (49–327)	0.175			
Prothrombin activity (%)[a]	99 (56–166)	100 (12–136)	0.829			
Total bilirubin (mg dl^{-1})[a]	0.7 (0.4–14.7)	0.7 (0.4–2.1)	0.815			
Aspartate aminotransferase (IU l^{-1})[a]	42 (14–2617)	56 (15–250)	<0.001	0.824		
Alanine aminotransferase (IU l^{-1})[a]	48 (11–2707)	65 (2–327)	0.018	0.809		
Lactate dehydrogenase (IU l^{-1})[a]	197 (123–899)	209 (43–473)	0.193			
Gamma glutamyl transpeptidase (IU l^{-1})[a]	37 (12–187)	47 (13–295)	0.049	0.928		
Albumin (g dl^{-1})[a]	4.3 (2.9–5.1)	4.2 (3.0–5.3)	0.376	0.200		
Total cholesterol (mg dl^{-1})[a]	174 (122–270)	173 (100–312)	0.161			
Triglycerides (mg dl^{-1})[a]	102 (33–2466)	97 (35–517)	0.861			
Glucose (mg dl^{-1})[a]	97 (68–334)	104 (70–284)	0.092	0.456		
HCV RNA (log IU ml^{-1})[a]	6.3 (4.2–7.9)	6.2 (4.2–7.5)	0.060	0.101		
Core 70 (wild:mutant)	35:14	42:25	0.325**			
Core 91 (wild:mutant)	20:29	34:33	0.290**			
ISDR (0:≥1)	14:34	24:42	0.421**			
IL28B (TT:TG or GG)	64:12	52:25	0.016**	0.011	3.000[b]	1.282–7.019
Fibrosis (F0–1:F2–3)	33:43	26:51	0.220**			
Inflammatory activity (A0–1:A2–3)	25:50	16:61	0.081**	0.066		

Univariate analysis was performed with Mann–Whitney U test and **chi-square test

Multiple logistic regression analysis was performed using variables that were significant ($P < 0.05$) or marginally significant ($P < 0.10$) in univariate analysis

[a] Median (range)

[b] IL28B genotypes were coded as 0 or 1 depending on whether the subject carried the minor allele

Table 4 Association between fatty degeneration and IL28B genotype

	IL28B		Univariate analysis
	TT	TG or GG	P value
Obesity group (BMI ≥25 kg m^{-2}, $N = 36$)			
Vesicular change ratio (<0.002:≥0.002)	12:19	2:3	1.000*
Clear cell change ratio (<0.033:≥0.033)	20:11	2:3	0.357*
Non-obesity group (BMI <25 kg m^{-2}, $N = 114$)			
Vesicular change ratio (<0.002:≥0.002)	52:30	9:23	0.001
Clear cell change ratio (<0.033:≥0.033)	48:34	10:22	0.009

Univariate analysis was performed with chi-square test and *Fisher's exact test

analysis using the Mann–Whitney U test, the IL28B genotype was found to be significantly associated with clear cell change and vesicular change ($P = 0.001$, $P < 0.001$, respectively). When continuous values were used in multiple regression, the association between IL28B genotype and fatty degeneration was also observed. *IL28B* genotype, HCV RNA titer and liver fibrosis stage were identified as independent factors for vesicular change ($P = 0.003$, $P = 0.022$, $P = 0.047$, respectively), and the *IL28B* genotype was identified as an independent factor for clear cell change ($P < 0.001$). Genotypes of rs738409 within the Patatin-like phospholipase domain-containing 3 (PNPLA3) locus were also recently reported to be associated with hepatic steatosis in chronic hepatitis C patients

(odds ratio 1.90–2.55) [38–40]. It would be interesting to analyze the effect of the PNPLA3 genotype on fatty degeneration in the present study; however, given the small number of study subjects and the small odds ratios reported in these studies, this study lacks the statistical power to verify the association between hepatic steatosis and PNPLA3.

Chronic HCV infection is known to be associated with fatty change of the liver, and the incidence of fatty change in chronic hepatitis C patients is higher than in those with other chronic liver dysfunctions [36, 41]. The mechanisms of fatty change in chronic hepatitis C patients are still unclear, but the induction of liver steatosis was observed in the presence of the HCV core protein in vitro and in vivo. In a transgenic mouse study, all the male and approximately 50% of the female mice developed liver steatosis by the age of 6 months [42]. Furthermore, the HCV core transfected cells were shown to activate the deposition of lipid [36, 37, 41, 43]. Thus it was hypothesized that chronic HCV infection might be associated with fatty change and the effect of clinical background. As shown in Tables 2 and 3, hepatic histological changes, including both vesicular and clear cell change, were significantly associated with BMI, aspartate aminotransferase, γ-GTP and HCV RNA levels in univariate analysis, whereas clear cell change was not associated with BMI. As shown in Fig. 2, clear cell change was strongly related to HCV infection, whereas it was rarely observed in the liver tissues of patients with non-alcoholic fatty liver disease. These findings suggest that vesicular change is associated with obesity or other lipid depositions, and that clear cell change is associated with chronic HCV infection.

Recently, several groups have reported significant associations between several linked SNPs in the *IL28B* locus and HCV eradication with IFN therapy based on genome-wide association analysis. The sustained virological response rate in chronic hepatitis C patients homozygous for the major allele (genotypes rs8099917 TT or rs12980275 CC or rs12979860 CC) was significantly higher than in patients heterozygous or homozygous for the minor allele [24–27]. Serum γ-GTP levels and liver histological fibrosis and inflammation levels in chronic hepatitis C patients with the favorable TT or CC SNP genotypes were also significantly lower than in those with the minor genotypes [28]. Although other host factors, such as liver steatosis or insulin resistance, have been demonstrated to be associated with virological response [23, 44], this study demonstrates that SNPs in the *IL28B* locus might affect steatosis in chronic hepatitis C patients. As the influence of the *IL28B* genotype was observed with both clear cell change and vesicular change (Tables 2, 3), and these associations became more remarkable in the non-obese group (Table 4), it is tempting to speculate that differences in IL28B expression might cause an aberration of lipid metabolism in chronic hepatitis C patients. An association between IL28B genotype at rs12979860 and hepatic steatosis in chronic hepatitis C patients was demonstrated in a previous report [45]. The results of this study were very similar given the strong association between the rs8099917 and rs12979860 genotypes [35], but the methods used to evaluate hepatic steatosis were quite different. In the previous report, hepatic steatosis was subjectively evaluated by pathologists using the Brunt classification, whereas in the present study, hepatic steatosis was evaluated objectively using a quantitative method, and two different classes of steatotic change, clear cell change and vesicular change were analyzed separately.

In conclusion, the relationship between clinical background and fatty change in liver tissue was analyzed using an operator-independent method, and significant associations between fatty change level and *IL28B* genotypes or HCV RNA level were identified. These findings suggest that these factors are connected to an aberration of lipid metabolism in chronic hepatitis C patients.

Acknowledgments The authors thank Rie Akiyama for technical assistance and Aya Furukawa for clerical assistance. This study was supported by Grants-in-Aid for Scientific Research and Development from the Ministry of Education, Sports, Culture and Technology, and in part by a Grant-in-Aid from the Ministry of Health, Labor and Welfare of Japan, and was carried out at the Research Center for Molecular Medicine, Faculty of Medicine, Hiroshima University, and the Analysis Center of Life Science, Hiroshima University.

Conflict of interest None.

References

1. Alter HJ, Purcell RH, Shih JW, et al. Detection of antibody to hepatitis C virus in prospectively followed transfusion recipients with acute and chronic non-A, non-B hepatitis. N Engl J Med. 1989;321:1494–500.
2. Cooper S, Erickson AL, Adams EJ, et al. Analysis of a successful immune response against hepatitis C virus. Immunity. 1999;10:439–49.
3. Lee SH, Kim YK, Kim CS, et al. E2 of hepatitis C virus inhibits apoptosis. J Immunol. 2005;175:8226–35.
4. Akuta N, Chayama K, Suzuki F, et al. Risk factors of hepatitis C virus-related liver cirrhosis in young adults: positive family history of liver disease and transporter associated with antigen processing 2(TAP2)*0201 Allele. J Med Virol. 2001;64:109–16.
5. Dusheiko GM. The natural course of chronic hepatitis C: implications for clinical practice. J Viral Hepat. 1998;5(Suppl 1):9–12.
6. Ikeda K, Saitoh S, Suzuki Y, et al. Disease progression and hepatocellular carcinogenesis in patients with chronic viral hepatitis: a prospective observation of 2215 patients. J Hepatol. 1998;28:930–8.
7. Kenny-Walsh E. Clinical outcomes after hepatitis C infection from contaminated anti-D immune globulin. Irish Hepatology Research Group. N Engl J Med. 1999;340:1228–33.

8. Niederau C, Lange S, Heintges T, et al. Prognosis of chronic hepatitis C: results of a large, prospective cohort study. Hepatology. 1998;28:1687–95.
9. Davis GL, Balart LA, Schiff ER, et al. Treatment of chronic hepatitis C with recombinant interferon alfa. A multicenter randomized, controlled trial. Hepatitis Interventional Therapy Group. N Engl J Med. 1989;321:1501–6.
10. Di Bisceglie AM, Martin P, Kassianides C, et al. Recombinant interferon alfa therapy for chronic hepatitis C. A randomized, double-blind, placebo-controlled trial. N Engl J Med. 1989;321:1506–10.
11. Davis GL, Esteban-Mur R, Rustgi V, et al. Interferon alfa-2b alone or in combination with ribavirin for the treatment of relapse of chronic hepatitis C. International Hepatitis Interventional Therapy Group. N Engl J Med. 1998;339:1493–9.
12. McHutchison JG, Gordon SC, Schiff ER, et al. Interferon alfa-2b alone or in combination with ribavirin as initial treatment for chronic hepatitis C. Hepatitis Interventional Therapy Group. N Engl J Med. 1998;339:1485–92.
13. Reichard O, Norkrans G, Fryden A, Braconier JH, Sonnerborg A, Weiland O. Randomised, double-blind, placebo-controlled trial of interferon alpha-2b with and without ribavirin for chronic hepatitis C. The Swedish Study Group. Lancet. 1998;351:83–7.
14. Schalm SW, Hansen BE, Chemello L, et al. Ribavirin enhances the efficacy but not the adverse effects of interferon in chronic hepatitis C. Meta-analysis of individual patient data from European centers. J Hepatol. 1997;26:961–6.
15. Fried MW, Shiffman ML, Reddy KR, et al. Peginterferon alfa-2a plus ribavirin for chronic hepatitis C virus infection. N Engl J Med. 2002;347:975–82.
16. Hoofnagle JH, Ghany MG, Kleiner DE, et al. Maintenance therapy with ribavirin in patients with chronic hepatitis C who fail to respond to combination therapy with interferon alfa and ribavirin. Hepatology. 2003;38:66–74.
17. Manns MP, McHutchison JG, Gordon SC, et al. Peginterferon alfa-2b plus ribavirin compared with interferon alfa-2b plus ribavirin for initial treatment of chronic hepatitis C: a randomised trial. Lancet. 2001;358:958–65.
18. Akuta N, Suzuki F, Hirakawa M, et al. A matched case-controlled study of 48 and 72 weeks of peginterferon plus ribavirin combination therapy in patients infected with HCV genotype 1b in Japan: amino acid substitutions in HCV core region as predictor of sustained virological response. J Med Virol. 2009;81:452–8.
19. Akuta N, Suzuki F, Kawamura Y, et al. Predictors of viral kinetics to peginterferon plus ribavirin combination therapy in Japanese patients infected with hepatitis C virus genotype 1b. J Med Virol. 2007;79:1686–95.
20. Akuta N, Suzuki F, Kawamura Y, et al. Predictive factors of early and sustained responses to peginterferon plus ribavirin combination therapy in Japanese patients infected with hepatitis C virus genotype 1b: amino acid substitutions in the core region and low-density lipoprotein cholesterol levels. J Hepatol. 2007;46:403–10.
21. Akuta N, Suzuki F, Kawamura Y, et al. Prediction of response to pegylated interferon and ribavirin in hepatitis C by polymorphisms in the viral core protein and very early dynamics of viremia. Intervirology. 2007;50:361–8.
22. Kitamura S, Tsuge M, Hatakeyama T, et al. Amino acid substitutions in core and NS5A regions of the HCV genome can predict virological decrease with pegylated interferon plus ribavirin therapy. Antivir Ther. 2010;15:1087–97.
23. Okanoue T, Itoh Y, Hashimoto H, et al. Predictive values of amino acid sequences of the core and NS5A regions in antiviral therapy for hepatitis C: a Japanese multi-center study. J Gastroenterol. 2009;44:952–63.
24. Ge D, Fellay J, Thompson AJ, et al. Genetic variation in IL28B predicts hepatitis C treatment-induced viral clearance. Nature. 2009;461:399–401.
25. Rauch A, Kutalik Z, Descombes P, et al. Genetic variation in IL28B is associated with chronic hepatitis C and treatment failure: a genome-wide association study. Gastroenterology 2010; 138:1338–45, 1345.e1–7.
26. Suppiah V, Moldovan M, Ahlenstiel G, et al. IL28B is associated with response to chronic hepatitis C interferon-alpha and ribavirin therapy. Nat Genet. 2009;41:1100–4.
27. Tanaka Y, Nishida N, Sugiyama M, et al. Genome-wide association of IL28B with response to pegylated interferon-alpha and ribavirin therapy for chronic hepatitis C. Nat Genet. 2009;41: 1105–9.
28. Abe H, Ochi H, Maekawa T, et al. Common variation of IL28 affects gamma-GTP levels and inflammation of the liver in chronically infected hepatitis C virus patients. J Hepatol. 2010;53:439–43.
29. Haraguchi A, Ogai Y, Senoo E, et al. Verification of the addiction severity index Japanese version (ASI-J) as a treatment-customization, prediction, and comparison tool for alcohol-dependent individuals. Int J Environ Res Public Health. 2009;6:2205–25.
30. Osaki Y, Tanihata T, Ohida T, et al. Decrease in the prevalence of adolescent alcohol use and its possible causes in Japan: periodical nationwide cross-sectional surveys. Alcohol Clin Exp Res. 2009;33:247–54.
31. Desmet VJ, Gerber M, Hoofnagle JH, Manns M, Scheuer PJ. Classification of chronic hepatitis: diagnosis, grading and staging. Hepatology. 1994;19:1513–20.
32. Akuta N, Suzuki F, Sezaki H, et al. Predictive factors of virological non-response to interferon-ribavirin combination therapy for patients infected with hepatitis C virus of genotype 1b and high viral load. J Med Virol. 2006;78:83–90.
33. Akuta N, Suzuki F, Sezaki H, et al. Association of amino acid substitution pattern in core protein of hepatitis C virus genotype 1b high viral load and non-virological response to interferon-ribavirin combination therapy. Intervirology. 2005;48:372–80.
34. Kato N, Hijikata M, Ootsuyama Y, et al. Molecular cloning of the human hepatitis C virus genome from Japanese patients with non-A, non-B hepatitis. Proc Natl Acad Sci USA. 1990;87:9524–8.
35. Ochi H, Maekawa T, Abe H, et al. IL-28B predicts response to chronic hepatitis C therapy—fine-mapping and replication study in Asian populations. J Gen Virol. 2011;92:1071–81.
36. Bach N, Thung SN, Schaffner F. The histological features of chronic hepatitis C and autoimmune chronic hepatitis: a comparative analysis. Hepatology. 1992;15:572–7.
37. Gordon A, McLean CA, Pedersen JS, Bailey MJ, Roberts SK. Hepatic steatosis in chronic hepatitis B and C: predictors, distribution and effect on fibrosis. J Hepatol. 2005;43:38–44.
38. Cai T, Dufour JF, Muellhaupt B, et al. Viral genotype-specific role of PNPLA3, PPARG, MTTP, and IL28B in hepatitis C virus-associated steatosis. J Hepatol. 2011;55:529–35.
39. Trepo E, Pradat P, Potthoff A, et al. Impact of patatin-like phospholipase-3 (rs738409 C>G) polymorphism on fibrosis progression and steatosis in chronic hepatitis C. Hepatology. 2011;54:60–9.
40. Valenti L, Alisi A, Nobili V. I148M PNPLA3 variant and progressive liver disease: a new paradigm in hepatology. Hepatology. 2011.
41. Lonardo A, Adinolfi LE, Loria P, Carulli N, Ruggiero G, Day CP. Steatosis and hepatitis C virus: mechanisms and significance for hepatic and extrahepatic disease. Gastroenterology. 2004;126: 586–97.
42. Moriya K, Yotsuyanagi H, Shintani Y, et al. Hepatitis C virus core protein induces hepatic steatosis in transgenic mice. J Gen Virol. 1997;78(Pt 7):1527–31.
43. Asselah T, Rubbia-Brandt L, Marcellin P, Negro F. Steatosis in chronic hepatitis C: why does it really matter? Gut. 2006;55: 123–30.

44. Kurosaki M, Matsunaga K, Hirayama I, et al. A predictive model of response to peginterferon ribavirin in chronic hepatitis C using classification and regression tree analysis. Hepatol Res. 2010;40: 251–60.

45. Tillmann HL, Patel K, Muir AJ, et al. Beneficial IL28B genotype associated with lower frequency of hepatic steatosis in patients with chronic hepatitis C. J Hepatol. 2011;55:1195–200.